A N A L O G M E T H O D S O F

N O N L I N E A R V I B R A T I O N A N A L Y S I S

Thesis by

Donald Theodore Greenwood

In Partial Fulfillment of the Requirements

For the Degree of

Doctor of Philosophy

California Institute of Technology

Pasadena, California

1951

ACKNOWLEDGMENTS

Acknowledgment of his advice and encouragement is due particularly to Dr. Gilbert D. McCann, under whose supervision this research was carried on. Mr. B.N. Locanthi was very helpful in advising on equipment and circuitry problems. Many thanks are also due Miss Dorothy Denhard for her help in the preparation of the photographs.

TABLE OF CONTENTS

ABSTRACT

This thesis presents methods by which electrical analogies can be obtained for nonlinear systems. The accuracy of these methods is investigated and several specific types of nonlinear equations are studied in detail.

In Part I a general method is given for obtaining electrical analogs of nonlinear systems with one degree of freedom. Loop and node methods are compared and the stability of the loop analogy is briefly considered.

Parts II and III give a description of the equipment and a discussion of its accuracy. Comparisons are made between experimental and analytic solutions of linear systems.

Part IV is concerned with systems having a nonlinear restoring force. In particular, solutions of Duffing's equation are obtained, both by using the electrical analogy and also by approximate analytical methods.

Systems with nonlinear damping are considered in Part V. Two specific examples are chosen: (1) forced oscillations and (2) self-excited oscillations (van der Pol's equation). Comparisons are made with approximate analytic solutions.

Part VI gives experimental data for a system obeying Mathieu's equation. Regions of stability are obtained. Examples of subharmonic, ultraharmonic, and ultrasubharmonic oscillations are shown.

PART I

INTRODUCTION

1. Vibrations of single degree of freedom systems

This thesis will be concerned with an analysis of vibrating systems with one degree of freedom. A typical example of such a system might be as shown in Fig. 1.01. A force $F(t)$ is applied to mass m. Due to the spring, an opposing force $k(x,t)x$ is applied to m. Also, an opposing force of friction $c(\dot{x},t)\dot{x}$ may act on mass m. The equation of motion for this case is

$$m\ddot{x} + c(\dot{x},t)\dot{x} + k(x,t)x = F(t) \tag{1}$$

In the usual linear case, $c(\dot{x},t)$ and $k(x,t)$ are constant. Vibrations of linear systems have been thoroughly studied, and we will not consider them in this paper except as a means of checking the accuracy of the methods used on nonlinear systems.

Vibrations of nonlinear systems, however, have not received such thorough treatment. This is not due to lack of interest in or importance of the problem. It is rather a result of: (1) the difficulty of generalizing the problem into a few types, each having an analytic solution, and (2) the absence, until relatively recently, of adequate experimental methods of attacking a variety of nonlinear problems wherein some of the parameters could be varied continuously.

This thesis will be concerned primarily with electric analog methods of analyzing some general types of nonlinear

second order differential equations. The methods will be illustrated by obtaining solutions for several specific non-linear equations.

2. Two types of electrical analogies

Electrical analogies of mechanical systems can be constructed on either the (1) loop or (2) node basis. The electrical analog of a single degree of freedom system is shown in Fig. 1.02. Using Kirchhoff's first law, the sum of the voltage drops around the loop is set equal to zero, or

$$L\ddot{q} + R\dot{q} + \frac{q}{C} = E(t) \tag{2}$$

This equation is identical in form with equation (1). The following quantities are seen to be analogous:

inductance-----mass

resistance-----damping coefficient

elastance-----spring constant

charge-----displacement

time-----time

voltage-----force

The electrical network that results when the analogy is formulated on the nodal basis is shown in Fig. 1.03. Setting the sum of the currents flowing away from the node equal to zero (according to Kirchhoff's second law), the following equation results:

$$\int \frac{e}{L}dt + \frac{e}{R} + \dot{e}C = i(t)$$

or

$$C\ddot{e} + G\dot{e} + \Gamma e = \frac{di(t)}{dt} \tag{3}$$

In this case the analogous quantities are

capacitance-----mass

conductance-----damping coefficient

inverse inductance-----spring constant

voltage-----displacement

time-----time

$\frac{di(t)}{dt}$-----force

Of course, these methods of obtaining electrical analogies for mechanical systems are applicable also for the case of systems having many degrees of freedom. Several authors have given an excellent treatment of this subject (1,3,4,5) and it is outside the scope of this thesis.

3. Nonlinear impedances

In the study of nonlinear differential equations using the loop analogy, one is naturally led to look for methods of obtaining impedances that are a function of charge or its time derivatives.

The most straightforward method is to find an impedance, such as a varistor, with the proper characteristics

and incorporate it into the circuit. This method has the advantage of simplicity but has the disadvantage that the nonlinearity (Z vs i curve) cannot be easily changed in shape nor multiplied by a constant. Also, in certain cases the limitation on power dissipation may be serious.

If a nonlinear feedback resistance is placed between the output and input terminals of a negative gain amplifier of high input impedance, the input impedance to the system will be a nonlinear resistance whose magnitude can be controlled by varying the amplifier gain. (See Fig. 1.04.)

A method of obtaining an impedance with the nonlinear characteristics of a varistor is shown in Fig. 1.05. For further details on these methods of obtaining nonlinear impedances, see a paper by McCann, Wilts and Locanthi on the subject.(6) This paper also shows a network of resistors, crystal diodes, and batteries for obtaining a straight-segment approximation to an R(i) in which the resistance is always positive and single-valued.

These methods are quite adequate for many cases in which nonlinear impedances are needed. They have the advantages of relative simplicity combined with an accurate enough representation for many purposes. The principal limitations are that the impedances are positive throughout the range and the voltage across the terminals is a single-valued function of the current. Also, the impedance is a function of its current only; i.e., it is not a function of time or of voltage, current, etc., in some other part of

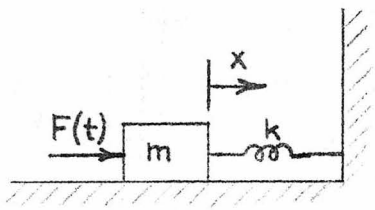

Fig. 1.01

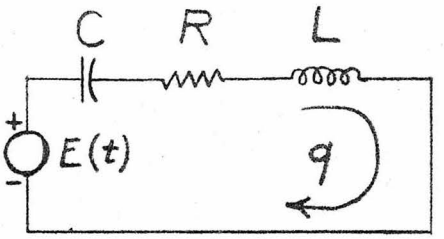

Fig. 1.02

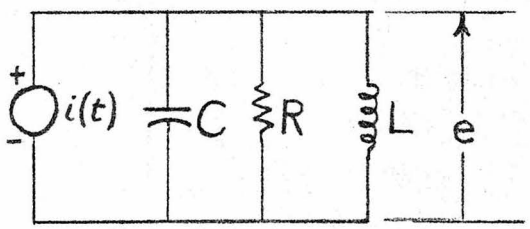

Fig. 1.03

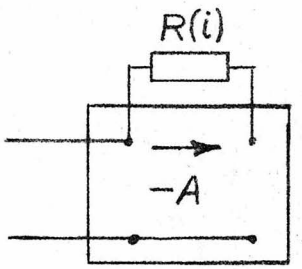

Fig. 1.04

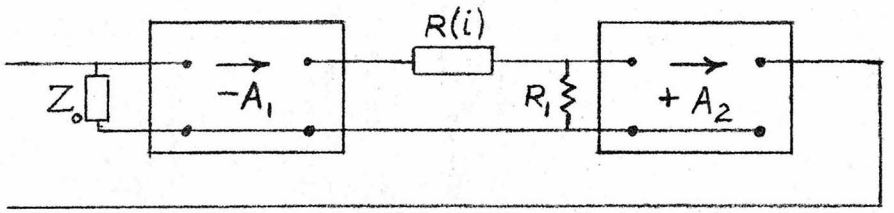

Fig. 1.05

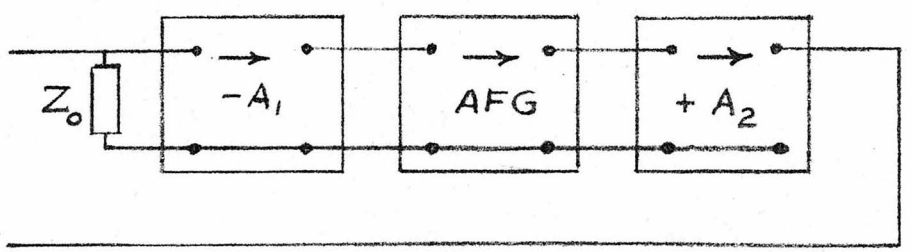

Fig. 1.06

the network.

An arbitrary function generator of the photoformer type has also been used as a two-terminal nonlinear impedance. (2,7) (See Part II for description of arbitrary function generator.) A circuit used for this purpose is shown in Fig. 1.06.

The photoformer type arbitrary function generator has the advantage of being able to act as a negative impedance. Also, the nonlinearities are rather conveniently determined by means of using the proper slide. However, the circuit shown has the disadvantage of requiring the mask to have an outline somewhat different from Z(i), the desired nonlinearity.

4. Loop analogies

In this section, loop analogies will be presented for the case of mechanical systems with one degree of freedom in which various types of nonlinearities occur in either the damping term or spring constant term. The inertial term could be made nonlinear by similar methods, but for mechanical systems this has little practical application. Coefficients that are a function of time are also considered. These circuits make use of an arbitrary function generator and, in some cases, a multiplier.

a. Damping a function of velocity

Suppose we wish the resistance between two points (A and G in Fig. 1.07) to be an arbitrary, single-valued

function $R_1(\dot{q})$ of the current. The input voltage to the arbitrary function generator is the voltage across a small resistor R'. It is thus directly proportional to the current flowing in the main loop. Therefore, the output voltage from the arbitrary function generator is a function of the loop current, and the voltage between A and G can be written

$$E_{AG} = R(\dot{q})\dot{q} \tag{4}$$

b. Damping a function of time

In this case, a multiplier is used in the feedback loop. (See Fig. 1.08.) One multiplier input is the voltage E_{AB} which, as before, is proportional to the loop current. The other input voltage is a function of time. The output voltage is given by

$$E_{AG} = R(t)\dot{q} \tag{5}$$

c. Spring constant a function of displacement

The voltage input to the arbitrary function generator is taken across a capacitor in this case (Fig. 1.09). Therefore, the output voltage is a function of the charge flowing in the main loop. The feedback voltage can be written as

$$E_{AG} = D(q)q \tag{6}$$

d. Spring constant a function of time

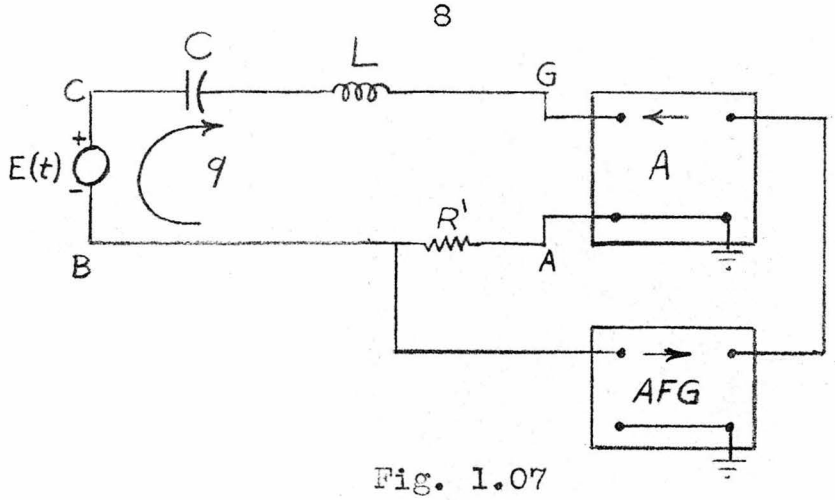

Fig. 1.07

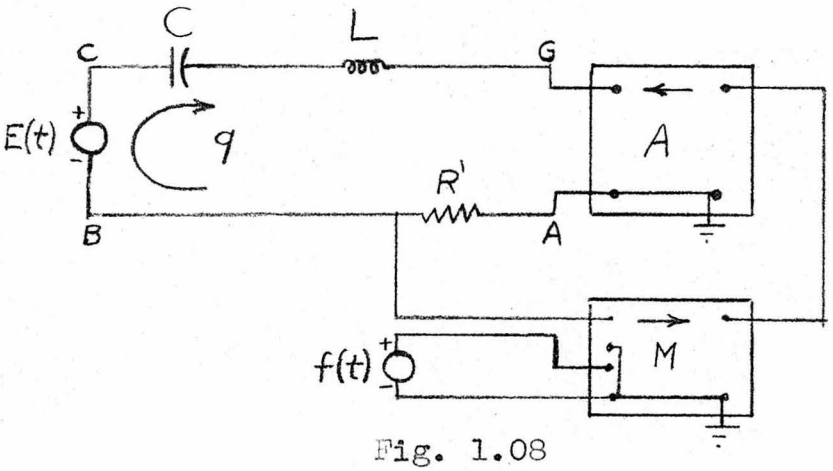

Fig. 1.08

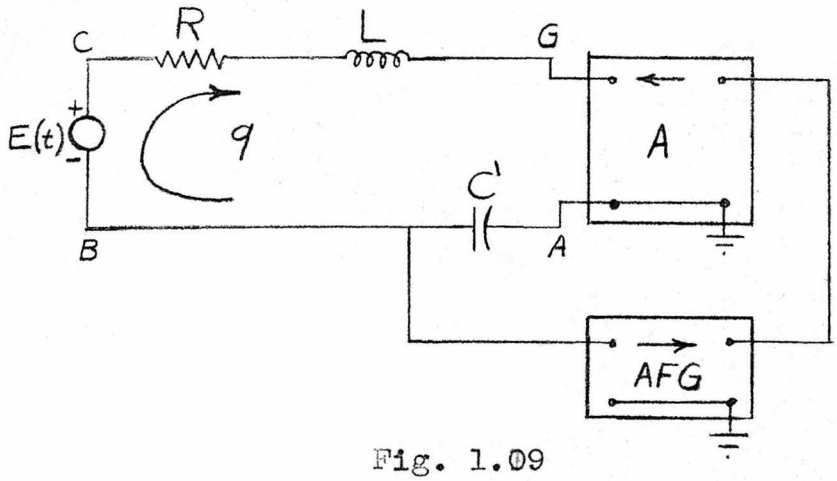

Fig. 1.09

The circuit for this case is given in Fig. 1.10. It is similar to (b) except that the voltage E_{AB} is taken from across a condenser instead of across a resistor.

(7) $$E_{AG} = D(t)q$$

e. Damping a function of displacement (Fig. 1.11)

Both an arbitrary function generator and a multiplier are necessary in this case. The input voltage to the arbitrary function generator is proportional to the loop charge, and the output voltage is used as one of the inputs to the multiplier. The other input voltage to the multiplier is proportional to loop current. This voltage is applied to the multiplier input that is capable of floating above ground. (See discussion of multiplier in Part II.) The voltage corresponding to the force of the nonlinear damper is given by

(8) $$E_{AG} = R(q)\dot{q}$$

f. Spring constant a function of velocity (Fig. 1.12)

The circuit for this case is found by methods analogous to those used in the previous paragraph. The voltage corresponding to the spring force is given by

(9) $$E_{AG} = D(\dot{q})q$$

5. Node analogies

Consider again the equation given previously for the

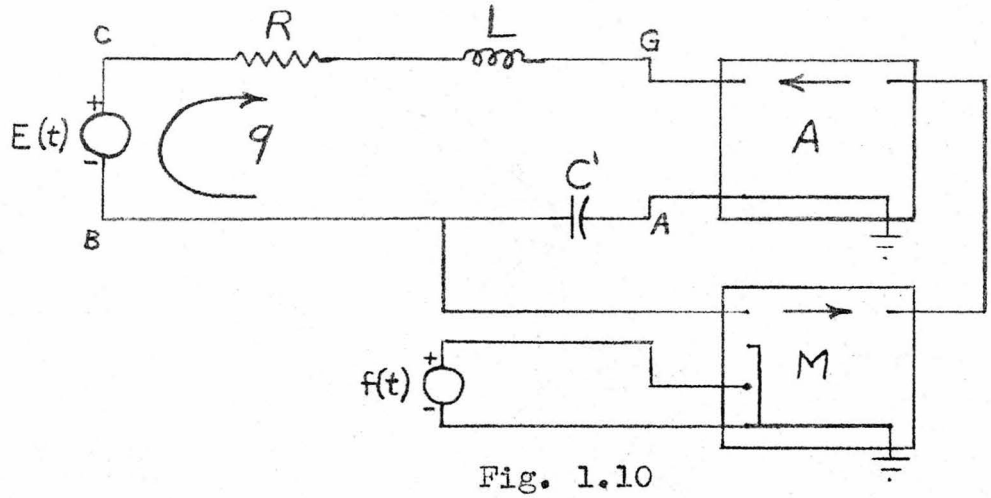

Fig. 1.10

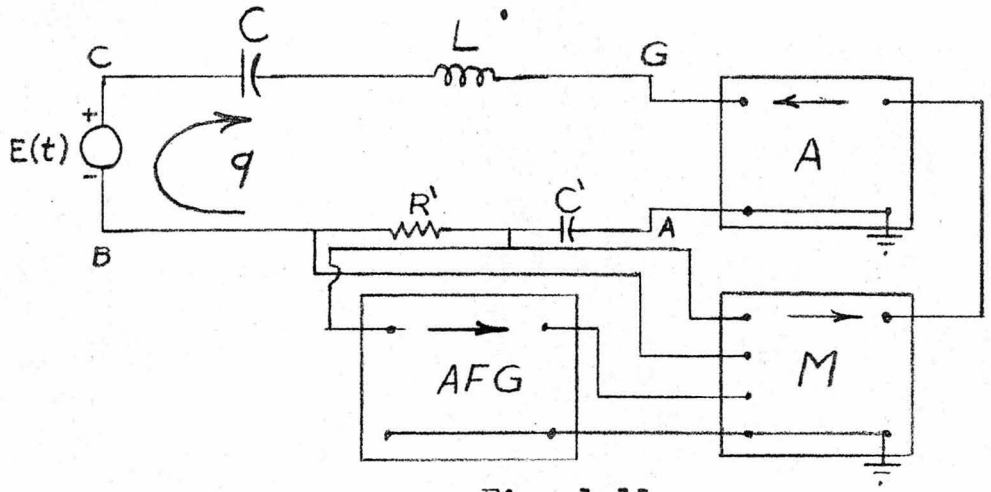

Fig. 1.11

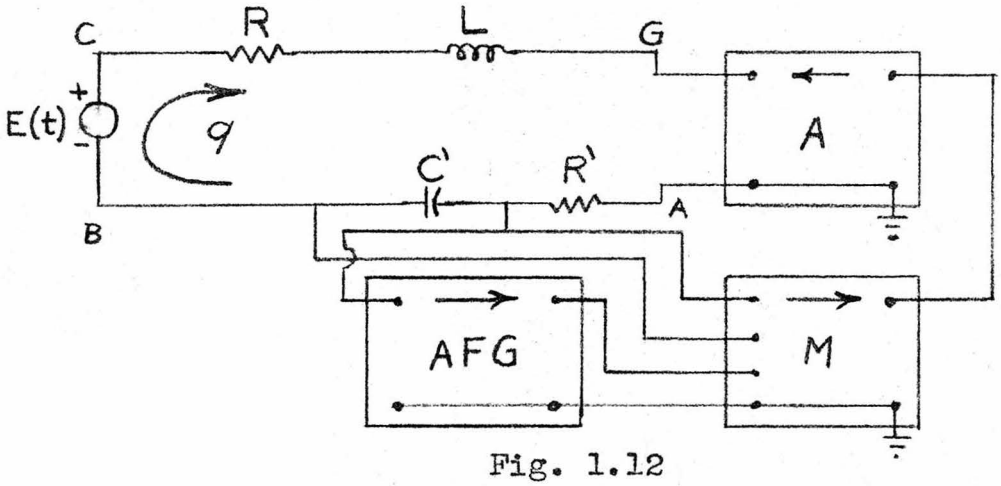

Fig. 1.12

node analogy.

$$C\ddot{e} + G\dot{e} + e = \frac{di(t)}{dt} \tag{10}$$

Recall that in the loop equations, a voltage proportional to q or $\dot{q}$ was taken from the loop, operated upon, and reintroduced as voltage E_{AG}. In the node analogy a voltage e or a voltage proportional to $\dot{e}$ is taken from the circuit, operated upon and used as the input to a current generator which, in turn, draws the required current from the node.

Suppose, for example, that an inverse inductance $\Gamma_1(e)$ is required. Fig. 1.13 shows the node analogy for the complete single degree of freedom mechanical system with a nonlinear spring. The input voltage to the arbitrary function generator is the node-pair voltage e. The output from the arbitrary function generator is $\Gamma_1(e)$ and the current drawn from node B by the current generator can be written

$$i_B = \Gamma(e)e \tag{11}$$

On the other hand, if we wish the damping to be a function of displacement, a more complicated type of nodal analogy is required. (See Fig. 1.14.) The input to the arbitrary function generator consists of the node-pair voltage e, as before. However, a voltage proportional to $\dot{e}$ is required as one input to the multiplier. This

voltage can be obtained from resistor R' for the case where the impedance of C' is much larger than R'. The current drawn from node B in this case is

$$i_B = G(e)\dot{e} \tag{12}$$

Using similar methods, node analogies could be developed for various types of nonlinear mechanical systems, as was done for the case of loop analogies.

6. A comparison of loop and node analogies

In representing the nonlinearities considered thus far, the input voltage to the arbitrary function generator has been proportional to either the displacement or velocity. By way of review, we shall list again the methods by which these voltages were obtained.

Loop analogy

q-----series condenser in loop

$\dot{q}$-----series resistor

Node analogy

e-----obtained directly

$\dot{e}$-----voltage across resistor of series condenser-resistor combination

It is seen that it is somewhat easier to obtain the required voltages from the circuit accurately in the case of the loop analogy. Particularly in the case of a voltage proportional to $\dot{e}$, inaccuracies in phase would occur due to the effect of the resistor R'.

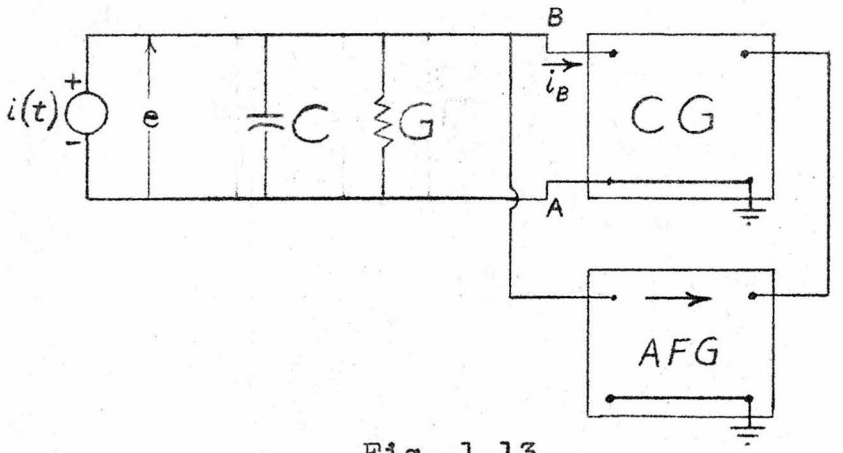

Fig. 1.13

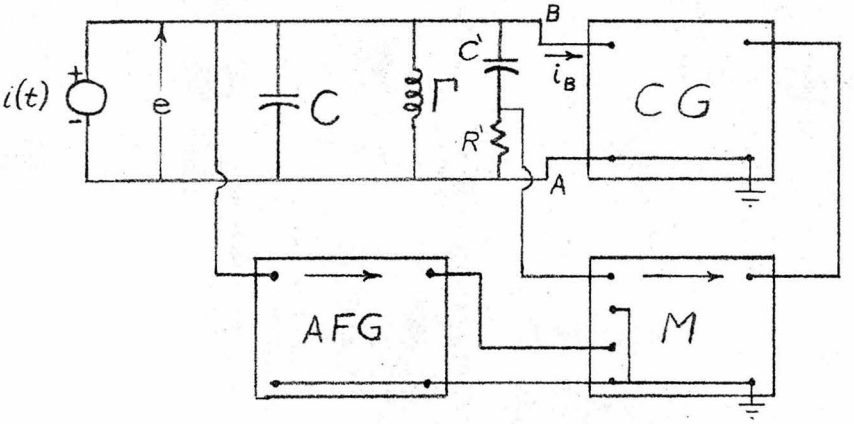

Fig. 1.14

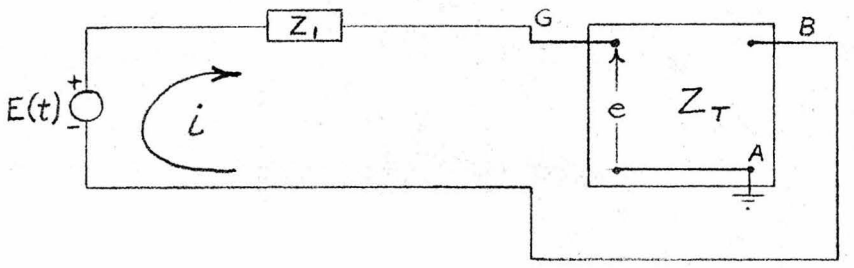

Fig. 1.15

Both methods of obtaining circuit voltages would seem to have a disturbing effect on the main circuit itself. In Part II a method is shown whereby these voltages can be obtained without appreciably affecting the circuit.

Another factor favoring the loop analogy is the fact that a voltage source of proper characteristics is more easily obtainable than the corresponding current source required for the node analogy.

For these reasons, the experimental investigations considered in this thesis have been carried on using the loop analogy.

7. Stability of the loop analogy

Next, let us consider the stability of the loop system shown in Fig. 1.15. Z_1 represents the impedance of the main loop at the frequency of the sinusoidal voltage source E(t). The four-terminal network represents the feedback loop. Assume that the input impedance to this network is very small and that the phase relationships are defined such that

$$e = iZ_T \tag{13}$$

The current flowing in the loop is also given by

$$i = \frac{E(t) - e}{Z_1} \tag{13.1}$$

Solving for e and i there results

(14) $$e = \frac{E(t)Z_T}{Z_1 + Z_T}$$

(15) $$i = \frac{E(t)}{Z_1 + Z_T}$$

Therefore, instability will occur at a particular frequency if

(16) $$Z_1 + Z_T = 0$$

Writing the loop transfer impedance in the form $Z_T = Ce^{A+iB}$, the conditions on phase B that cause instability are:

Z_1	B
inductive	-90°
resistive	180°
capacitive	90°

The amplitude and phase characteristics of the feedback loop, with and without the filter, are shown in Figs. 3.03 and 3.04. It is seen that oscillations are more likely to occur at a frequency above the main loop resonance where Z_1 is inductive and the feedback loop has greater phase shift.

The phase shift characteristics of the feedback loop were plotted on the basis of using the loop as a damper (i.e., coupling to the main loop by means of a resistor). If the coupling is by means of a condenser, an additional 90° lag must be introduced.

PART II

DESCRIPTION OF EQUIPMENT

1. The analog computer

The equipment used in the collection of data for this thesis consists of the California Institute of Technology Analog Computer. (See Fig. 2.01.) A general description of the computer has been given in several references (2,6,8) so the description given here will include only that equipment actually used in performing these experiments.

Since only single degree of freedom systems are considered, just a small fraction of the computer impedances were used. In those cases where a forcing function was required, a signal generator was used to drive an amplifier of low output impedance (2 ohms) which was connected across appropriate busses.

The usual computer metering circuits were used. Sinusoidal voltages were measured with a Ballantine voltmeter while voltages of non-sinusoidal shape were measured with an oscilloscope, being careful to keep the amplitude within the linear range of the scope.

2. Amplifiers

Two positive gain amplifiers were used in most of the analogies. These DC amplifiers have a one ohm output impedance and a continuously variable gain up to 100. They

17

can be operated above ground and can be easily adjusted to give zero DC output voltage. The current available at 200 volts peak to peak is 50 ma.

One amplifier was used for isolation between the arbitrary function generator and the main circuit. Usually a filter was used on the input to this amplifier, and thus the amplifier also served to isolate the filter from the impedance elements of the main circuit.

The other amplifier was used for the purpose of enabling one to take from the main loop voltages corresponding to displacement, velocity, etc. without having these voltages influence the operation of the loop itself. This was accomplished by using the circuit shown in Fig. 2.02. The gain of the amplifier is set to 1. In this case the output is equal to the input in phase and amplitude, and there is zero voltage between A and B. Therefore, the amplifier looks like a zero impedance to the loop. However, the loop current must follow the path AFB in flowing from A to B, and a voltage appears across AF which may be used as an input to other apparatus such as an arbitrary function generator.

3. Multiplier

The multiplier is a device whose output is the instantaneous product of two input voltages. The two inputs have impedances of 350 ohms and 500,000 ohms. The low impedance input is isolated from the system ground. The input signals to the multiplier have been limited to about 0.5 volts.

The amplitude response is uniform within 0.1 db from zero to 10,000 cps, and the phase shift is linear within this range and is 1.8° per kilocycle. The accuracy of the multiplier is such that the error is less than 1% of the maximum product (i.e., for case of maximum inputs).

The drift in the multiplier proved to be negligible. However, balance controls are provided to insure that the output is zero if either input is shorted.

A more complete description of the multiplier may be found in reference (8).

4. Arbitrary function generator

The arbitrary function generator is a device whose output voltage is an arbitrary function (normally single-valued) of the input voltage. It operates on the photoformer principle. The particular model used in these experiments is an improved version of those that have been in use for several years; however, the basic principle of operation remains unchanged. (7)

A schematic diagram of the arbitrary function generator is shown in Fig. 2.03. An opaque mask with the outline $y = f(x)$ is placed as a slide in front of the 3-inch cathode ray tube. If the feedback loop were open, the spot would rest near the top of the screen. However, when feedback loop is closed, the light from the spot falling on the phototube causes a voltage to be applied to the vertical plates, moving the spot downward. The gain is such that equilibrium

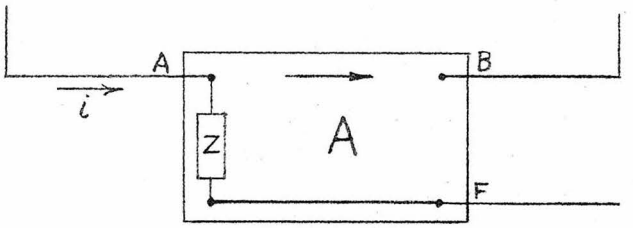

Fig. 2.02

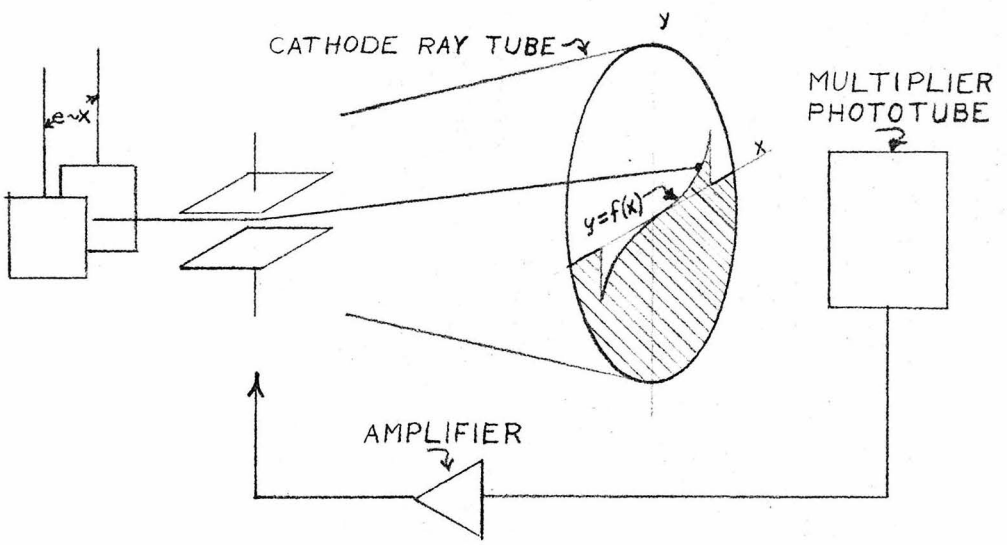

Fig. 2.03

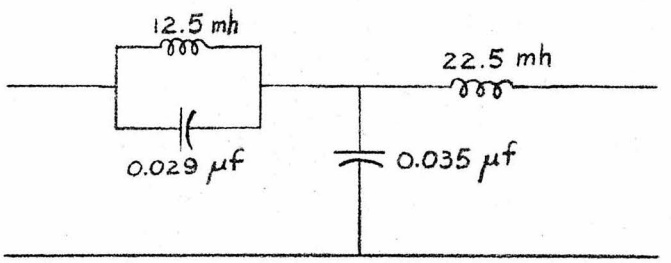

Fig. 2.04

occurs when the spot is partially obscured. When the beam is deflected by a voltage applied to the horizontal plates, the spot follows the edge of the mask. Therefore, if a voltage proportional to x is applied to the horizontal plates, the voltage applied to the vertical plates will be proportional to f(x). This voltage applied to the vertical plates is passed through an isolating amplifier and constitutes the output of the arbitrary function generator. In order to obtain increased accuracy, the gain of the feedback amplifier is quite high when the beam is near the center of the screen. However, the vertical deflection voltage is clipped at a level such that the spot will not leave the screen entirely and become "invisible" to the phototube. The usual working area of the cathode ray tube screen is a portion about 1 inch (vertical) by 2 inches (horizontal), and the scale of the mask is chosen to use this area as fully as possible.

The arbitrary function generator is equipped with an input potentiometer and output attenuator so that the mask can be used to best advantage without losing control of the overall gain.

The input impedance of the arbitrary function generator is 50K, and the output impedance is 1 ohm. The phase shift occurs primarily in the input potentiometer and thus is affected considerably by the potentiometer setting. With the input potentiometer at its maximum setting, the phase shift is negligible up to 2000 cps. Even at lower settings the

phase shift is not over 1° at 2000 cps, providing the arbitrary function generator is properly adjusted.

5. Filter

For many of the measurements a low-pass filter was used between the arbitrary function generator and the amplifier. The purpose of the filter is to permit the use of higher gains in the feedback loop without oscillation. (See Section 7, Part I.) The frequency range of the forcing functions was 200-2000 cps. Since the phase shift of the feedback loop without a filter increases to 180° at about 30 kc, there is a tendency for oscillation at about this frequency. (See Fig. 3.04.) A considerably higher loop gain can be used with a filter. For example, it was found that the maximum damping without oscillation (using linear slide) was $\zeta = 7.8$ with the filter as compared to $\zeta = 1.7$ without the filter. A comparison of amplitude and phase characteristics of the feedback loop with and without the filter is shown in Figs. 3.03 and 3.04. The filter used with the amplifier is shown in Fig. 2.04. It was chosen as the best compromise between the sharp cutoff characteristic of the m-derived filter and high attenuation throughout the cutoff range characteristic of the constant k type. Also, the phase shift of a constant k filter would be too great. A cutoff frequency of about 7 kc was chosen so that the amplitude and phase characteristics would be satisfactory below 2 kc, and yet the cutoff

frequency would be low enough to cause high attenuation in the higher phase shift regions.

PART III

ACCURACY OF EQUIPMENT

1. Effect of inductor shunt capacity

A large number of measurements were made for the purpose of checking the accuracy of the computer when it is connected as a linear system. Figs. 3.01 and 3.02 show the comparison of theoretical and experimental response curves, using an RLC series circuit. The magnitude of the series resistor was decreased with increasing frequency in order to compensate for the increasing inductor resistance. This correction was always made whenever response curves were obtained, either for linear or nonlinear systems.

It is seen that the theoretical and experimental values agree quite closely except that the amplitude seems to be consistently a little low at high frequencies. This is probably due to the fact that the inductor used in this case is self-resonant at $\beta = 3.5$ due to its shunt capacity. Now, the effective inductance of an LC parallel circuit (Fig. 3.10) is

(17) $$L_{eff} = \frac{L}{1 - \omega^2 LC}$$

(18) $$= \frac{L}{1 - \left(\frac{f}{f_o}\right)^2}$$

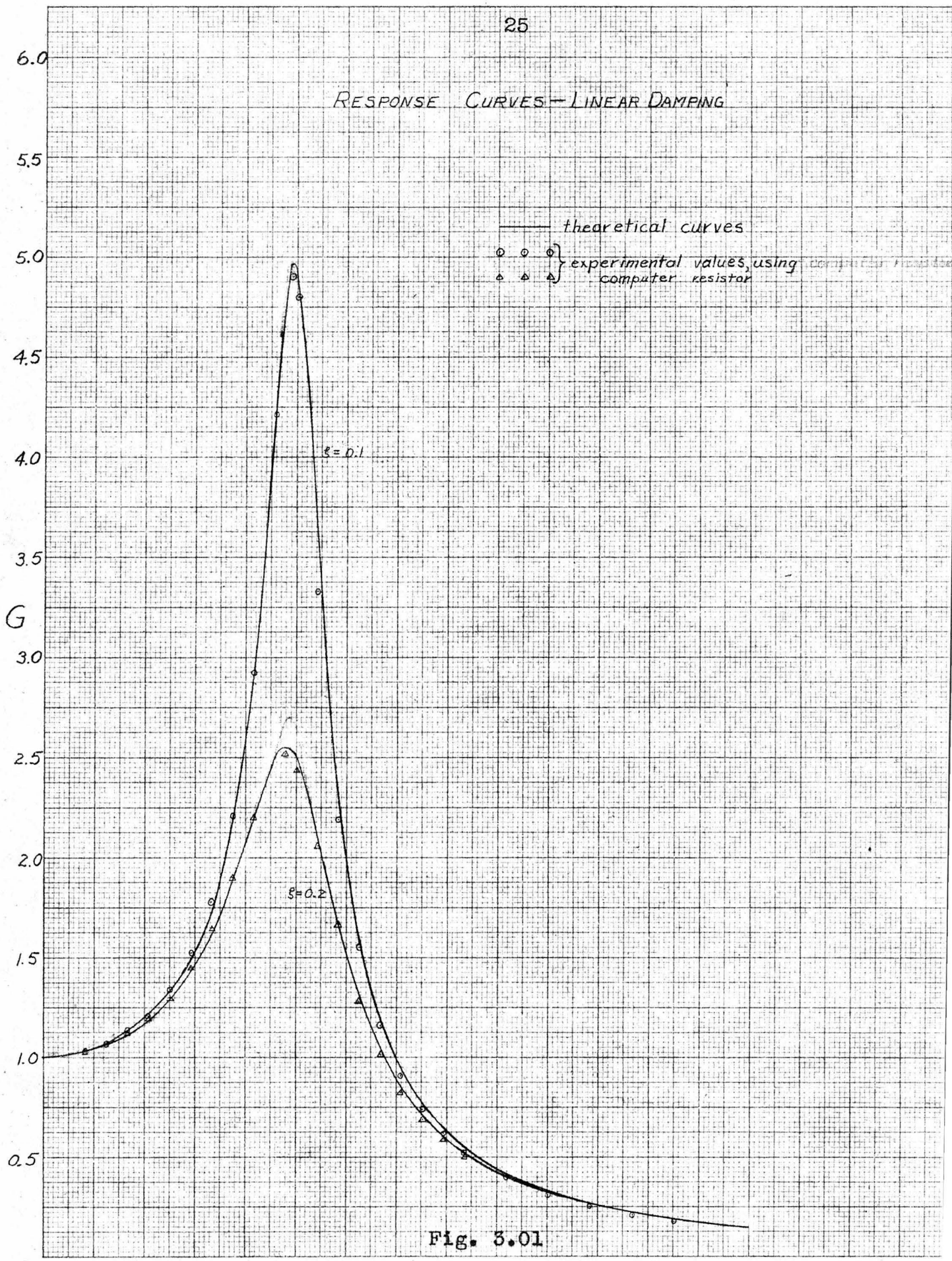

Fig. 3.01

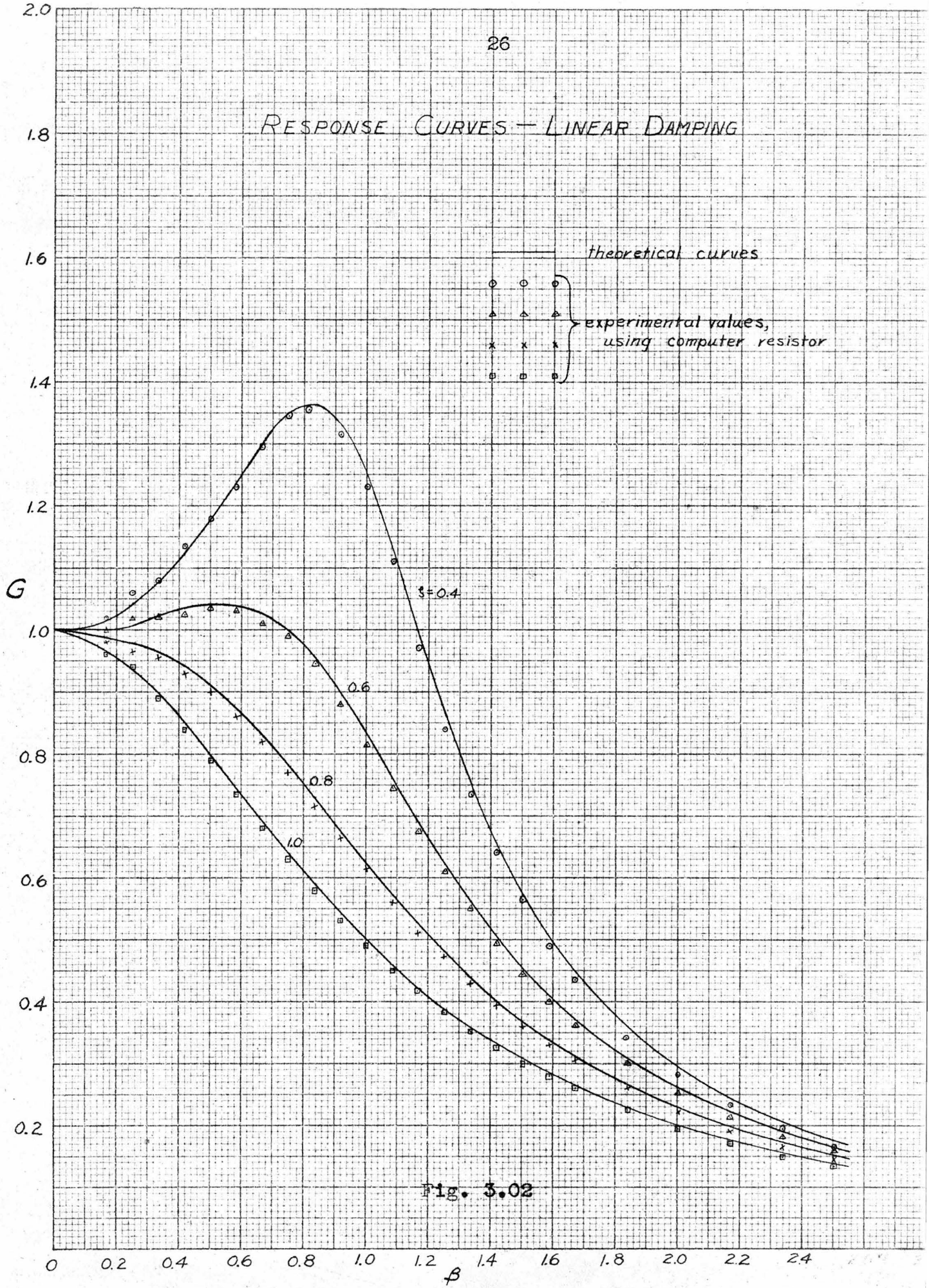

Fig. 3.02

where

$$f_o = \frac{1}{2\pi\sqrt{LC}}$$

In other words, the effective inductance increases as the self-resonant frequency is approached from below. This increased inductance will shift the system response curve to the left and thus decrease the amplitude at frequencies near the inductor self-resonance point.

The amplitude (voltage) measurements were made with a Ballantine voltmeter, and the frequency measurements were made by means of Lissajous figures using a 60-cycle source as reference.

2. Characteristics of feedback loop

Ideally, the feedback loop should have constant gain and zero phase shift for all frequencies. However, all measurements for this thesis are made at frequencies below 2 kc. Therefore, for our purposes, it is more profitable to attempt to approach this ideal as closely as possible in the region up to 2 kc. At higher frequencies, the gain and phase shift should be such as to provide the greatest stability consistent with the required loop gain.

Figs. 3.03 and 3.04 show the feedback loop characteristics, both with and without the filter. It is seen that the gain characteristics for frequencies less than 2000 cps are approximately the same in each case, but that the phase

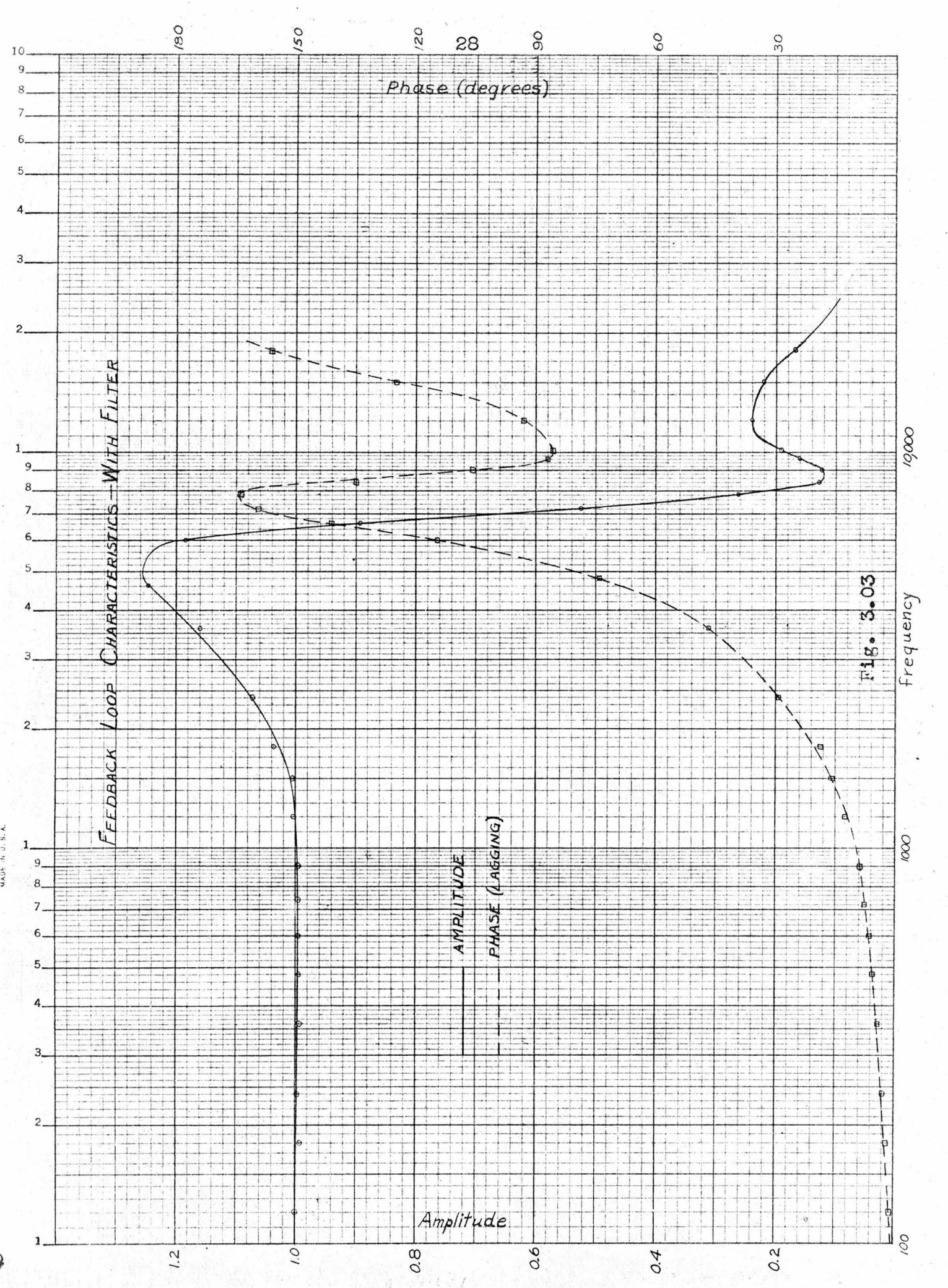

Fig. 3.03

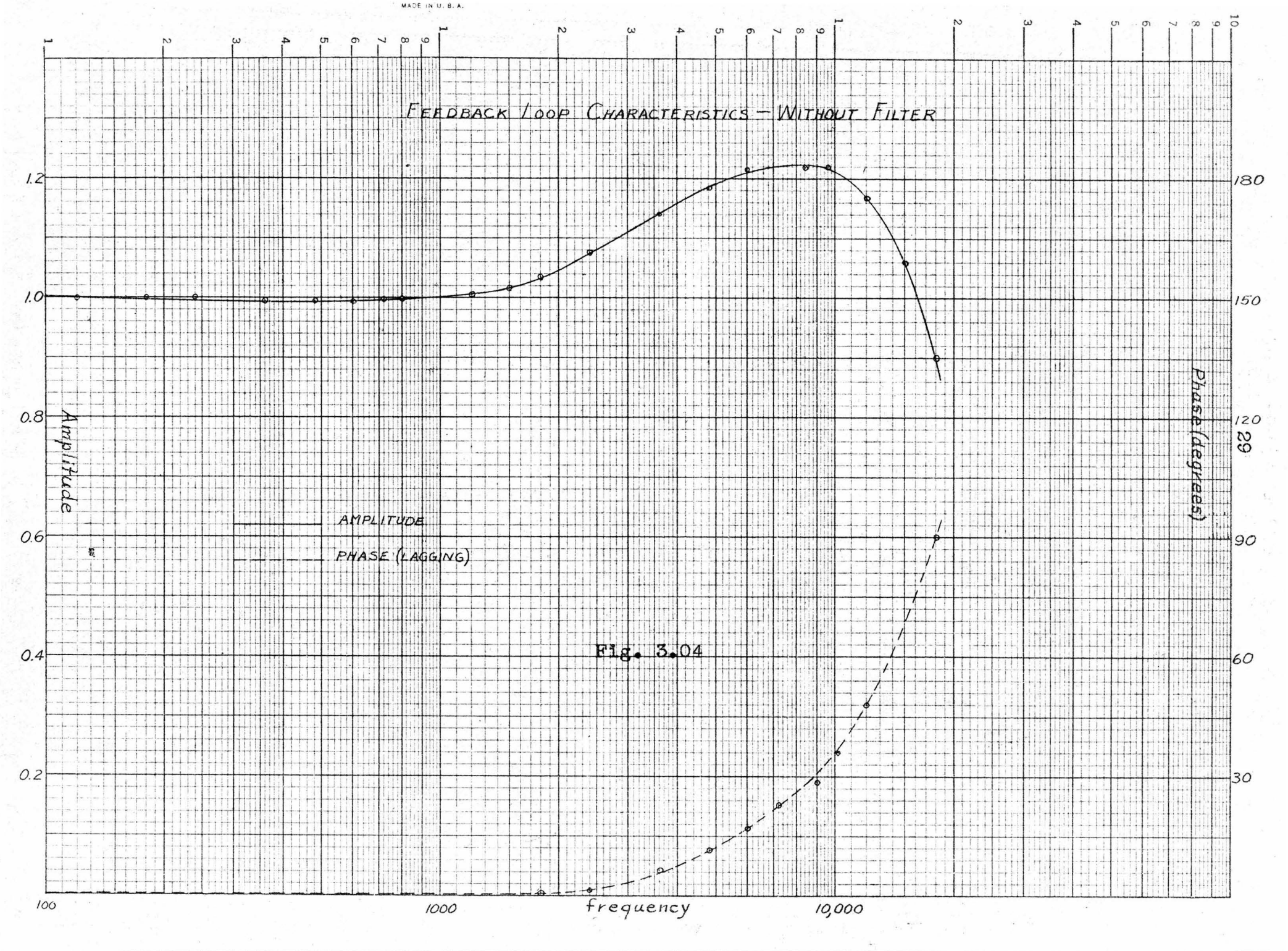

Fig. 3.04

shift is much greater with the filter.

The effect of a larger gain is that either the damping coefficient or spring constant is increased, depending upon whether the input voltage to the feedback circuit is taken from a resistor or condenser. In any event, increased gain merely increases the voltage applied to the system at AG. (See Fig. 3.13.)

Since the spring, damping and inertial forces are in phase with x, $\dot{x}$ and $\ddot{x}$, respectively, the phase relationships of these forces for steady-state forced linear vibrations are as shown in Fig. 3.11. With this figure the effect of phase shift in the feedback loop is more clearly seen.

3. The AFG used as a linear spring

For the case where the feedback loop is used as a linear spring (Fig. 3.12), the voltage AG will correspond to the spring force. Phase shift will cause the spring force to lag the damping force by more than 90° and thus will have a component corresponding to negative damping.

Let us consider more carefully the case where the phase shift varies linearly with frequency. The damping coefficient is proportional to the damping force per unit velocity or, in this case, the damping coefficient is proportional to the damping voltage per unit current. Now, for a given current, the voltage across the condenser is inversely proportional to frequency. Therefore, the negative damping coefficient due to phase shift is independent

of frequency. This fact makes it possible to correct for the phase shift directly by increasing slightly the value of the damping resistor.

Figs. 3.05 and 3.06 show the comparison of experimental data and the theoretical curves for the case where the feedback loop was used to represent a linear spring. It is seen that the experimental data form quite smooth curves. The main source of disagreement between experimental and theoretical values seems to be in the difficulty setting the various parameters exactly on their assigned values. (In this case the damping was slightly low for several curves.) On the other hand, the experimental curves are surprisingly accurate in their shape.

The transient response to a step function input is shown in Fig. 3.14 for three values of damping. The sinusoidal timing curves indicate the undamped natural frequency. In Fig. 3.14 (a) a slight irregularity can be noted in the trace. This is noticeable only for low damping (where the spring force is relatively large) and is due to a superimposed parasitic oscillation of higher frequency.

4. The AFG used as a linear damper

The feedback loop was set up as in Fig. 3.13 with a linear slide in the arbitrary function generator.

Looking at Fig. 3.11 it is seen that, when the feedback loop is used to give linear damping, a phase shift will give the effect of increasing the spring constant.

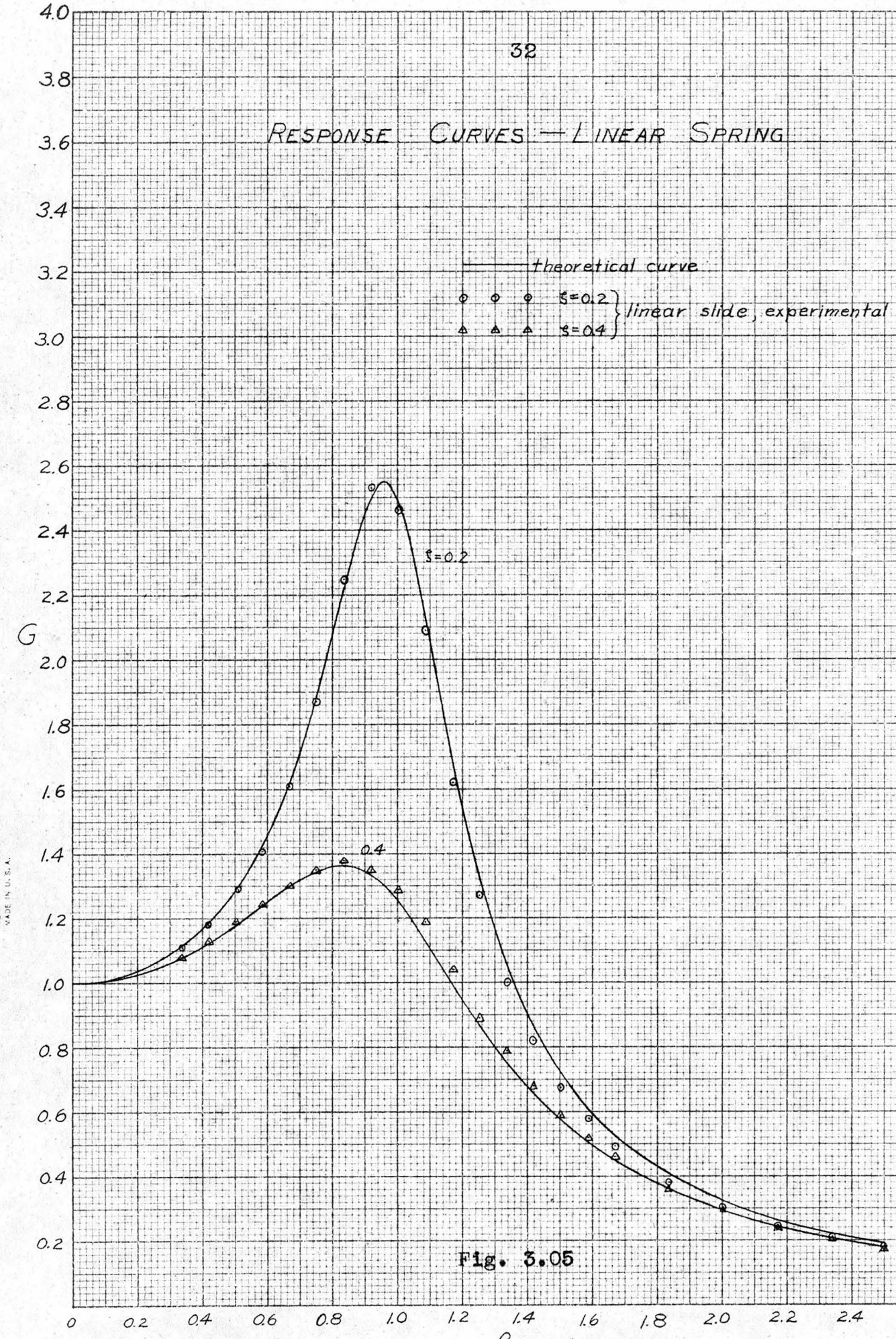

Fig. 3.05

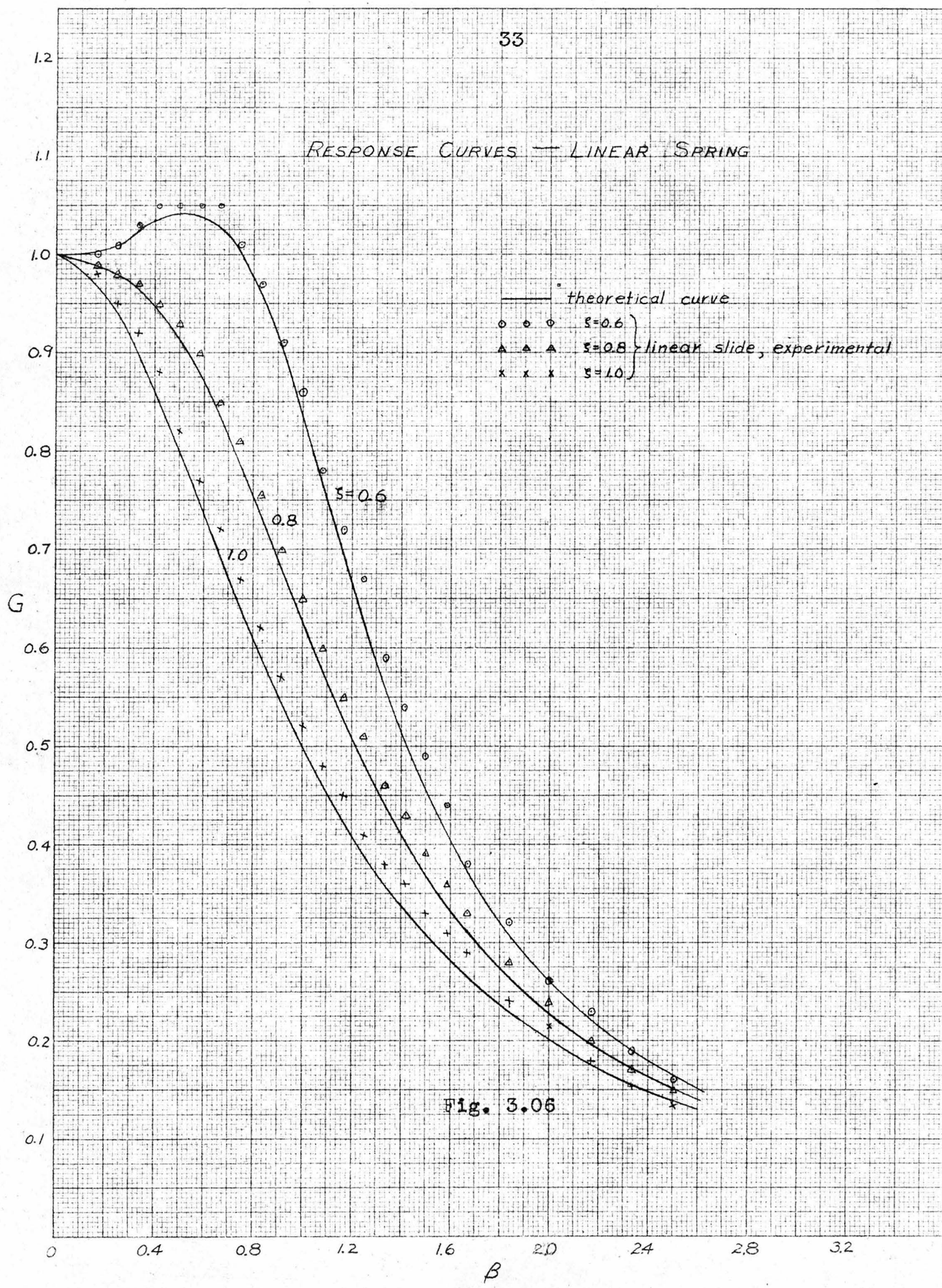

Fig. 3.06

Unfortunately, if phase shift varies linearly with frequency, the increase in the spring force will also vary linearly with frequency as opposed to the usual inverse variation. (This assumes constant current or velocity.) Therefore, in this case, one cannot make a correction for phase shift that will be good for a range of frequencies. The response curves for the case of linear damping are shown in Figs. 3.07, 3.08 and 3.09.

The comparison of experimental and theoretical results in this case shows good agreement at low values of damping with or without filter and also for higher damping with no filter. Note that the excessive falling off of amplitude at higher frequencies that appeared in previous cases (due to inductor shunt capacity) is not apparent here. In fact, the amplitude is somewhat too large at high frequencies for the case where the filter is used. This effect is due to phase shift in the feedback loop, causing an increased effective spring constant with the consequent higher resonant frequency. This increase of the apparent resonant frequency tends to make the amplitude larger for frequencies above resonance.

Fig. 3.15 shows the transient response to a step function input. The case of zero damping is obtained by adjusting the gain of the amplifier between A and B, Fig. 3.13, so that the total resistance of the main loop is zero. The damped high frequency oscillation that is apparent for the case $\zeta = 1.0$ is parasitic. Note that it accompanies the

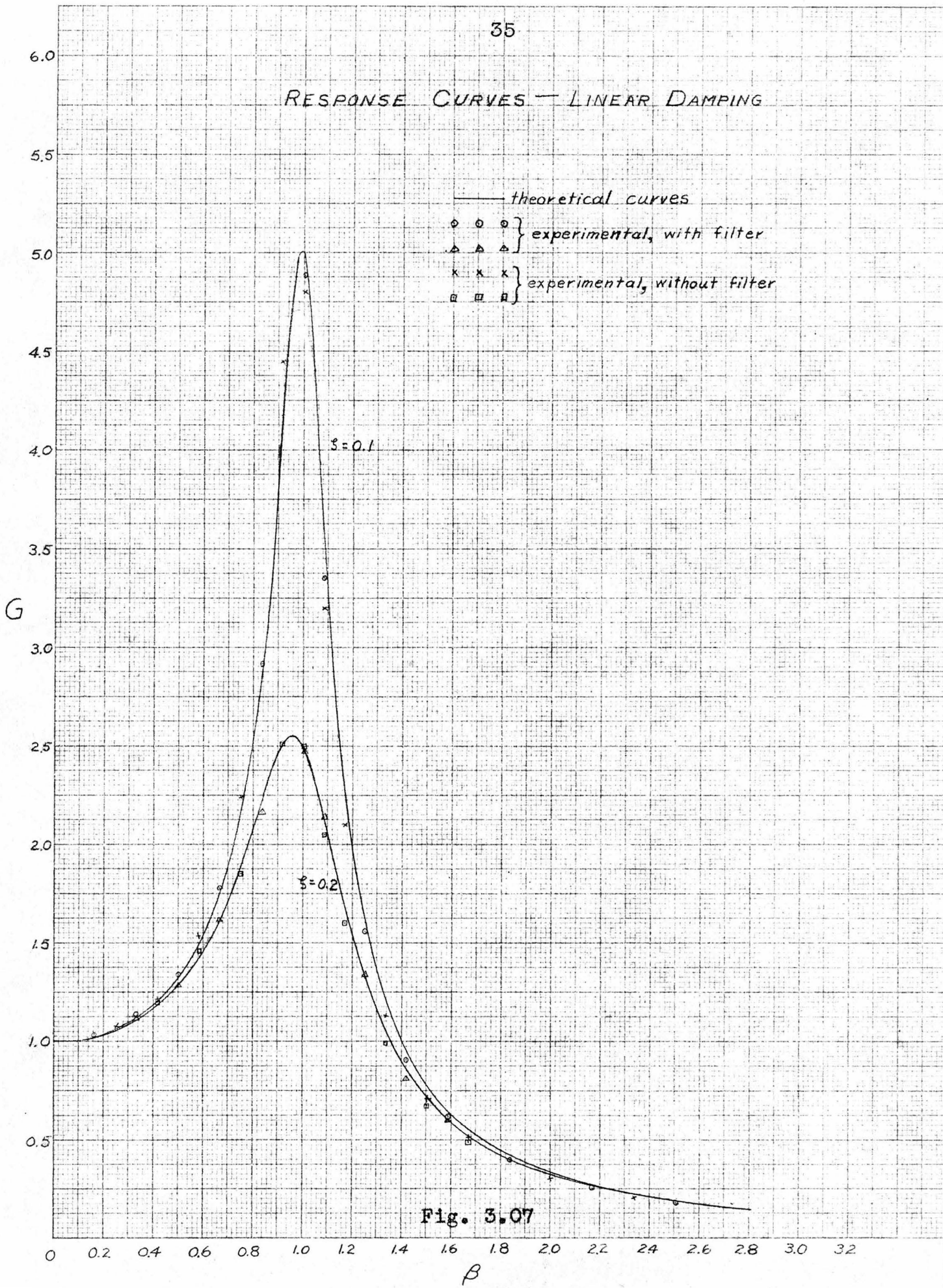

Fig. 3.07

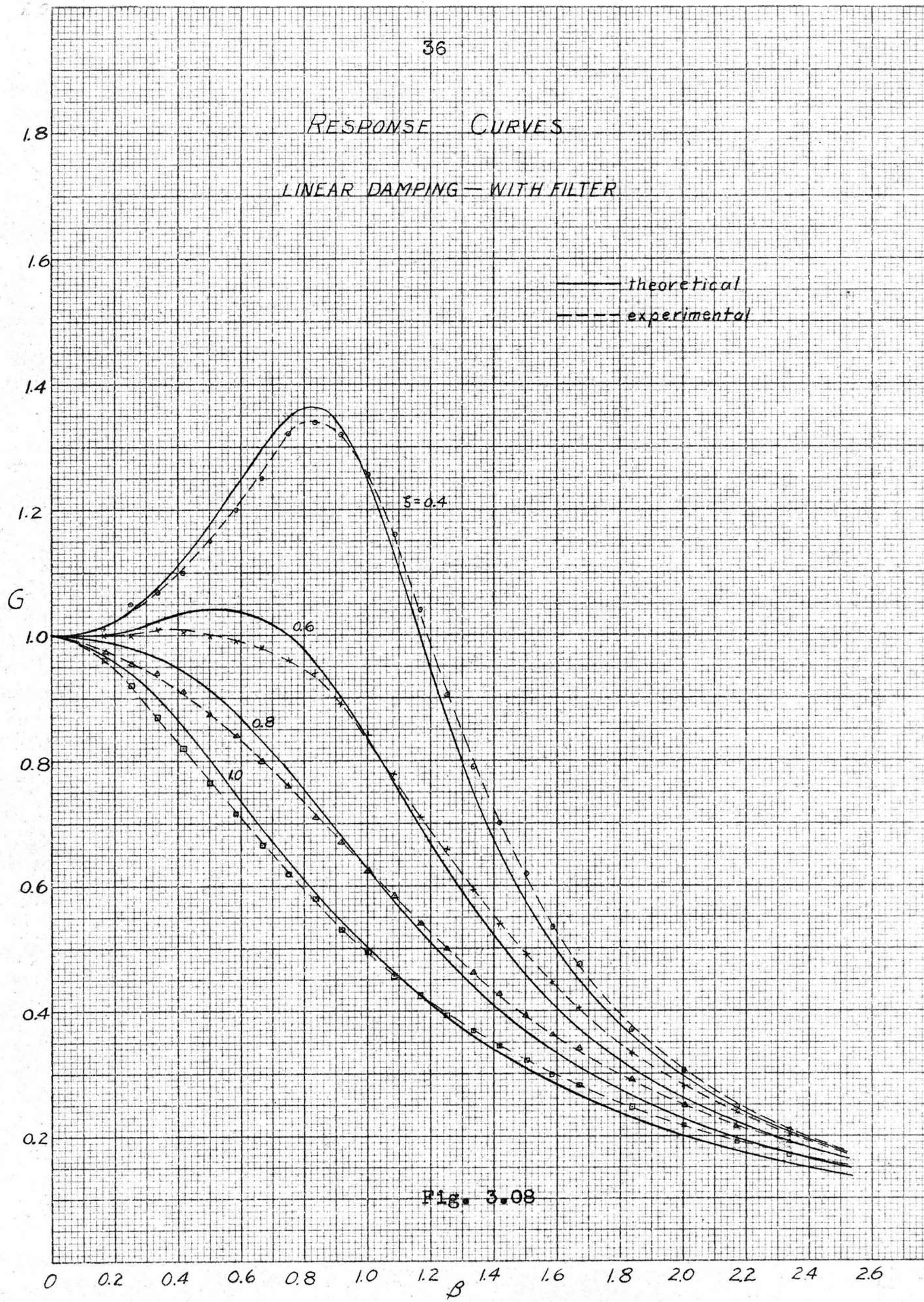

Fig. 3.08

RESPONSE CURVES

LINEAR DAMPING—WITHOUT FILTER

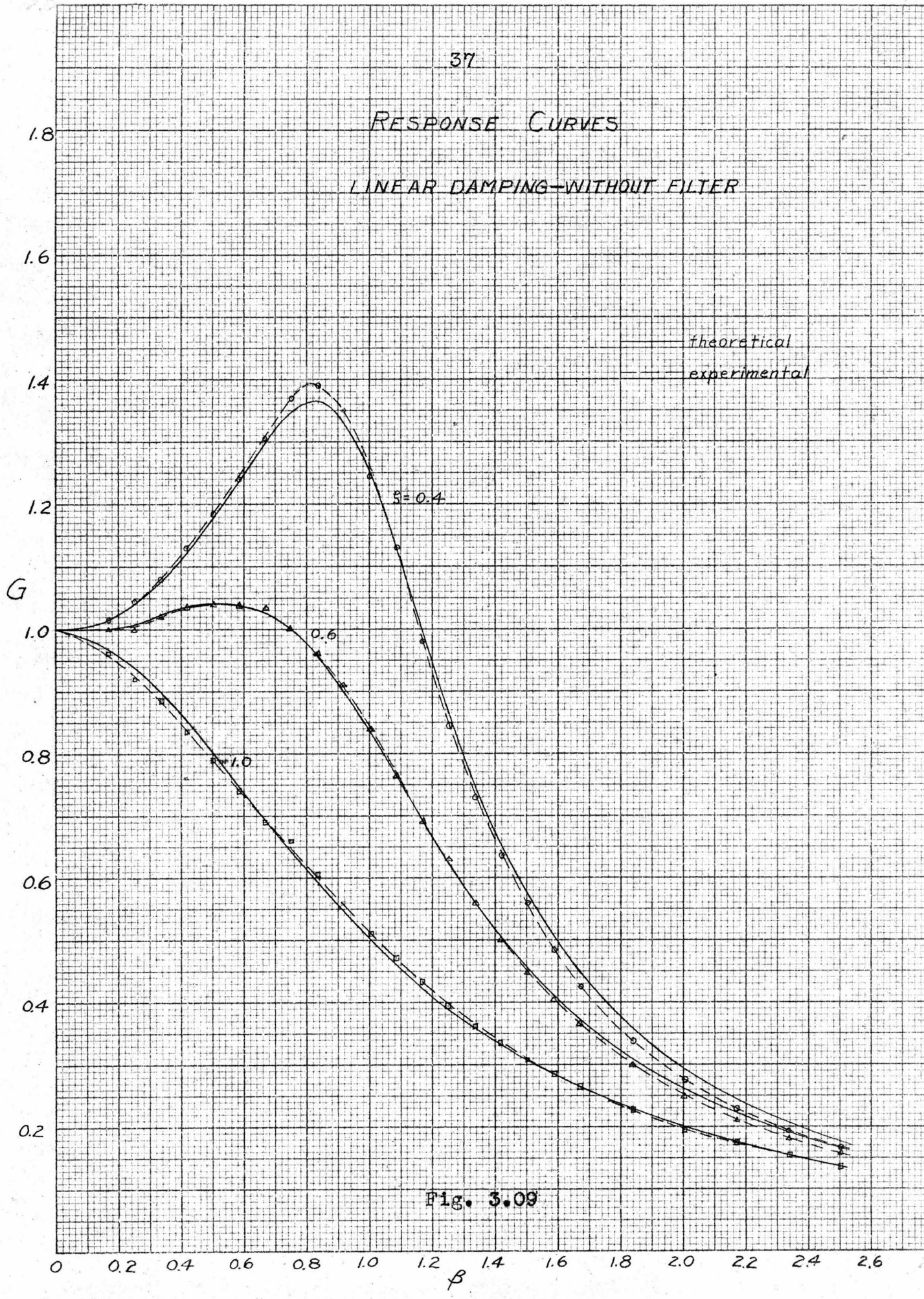

Fig. 3.09

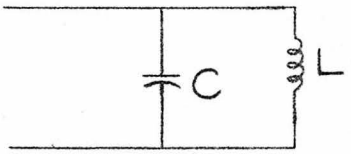

Fig. 3.10

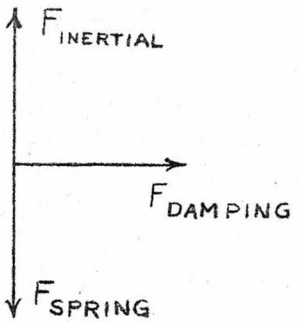

Fig. 3.11

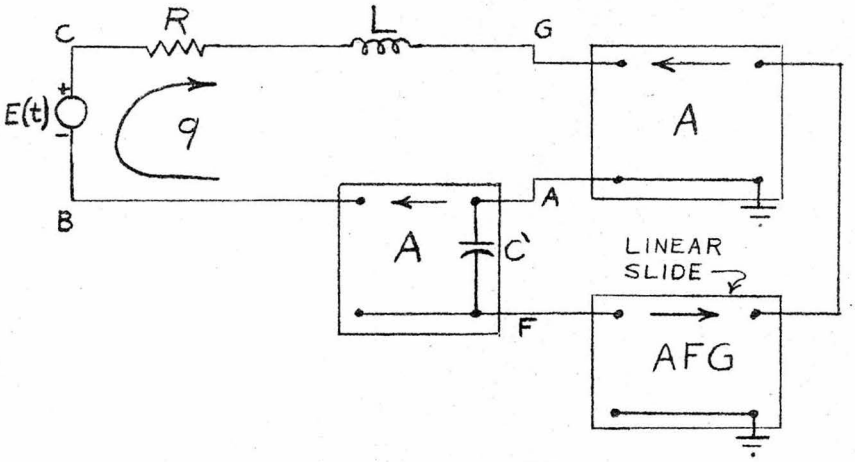

Fig. 3.12

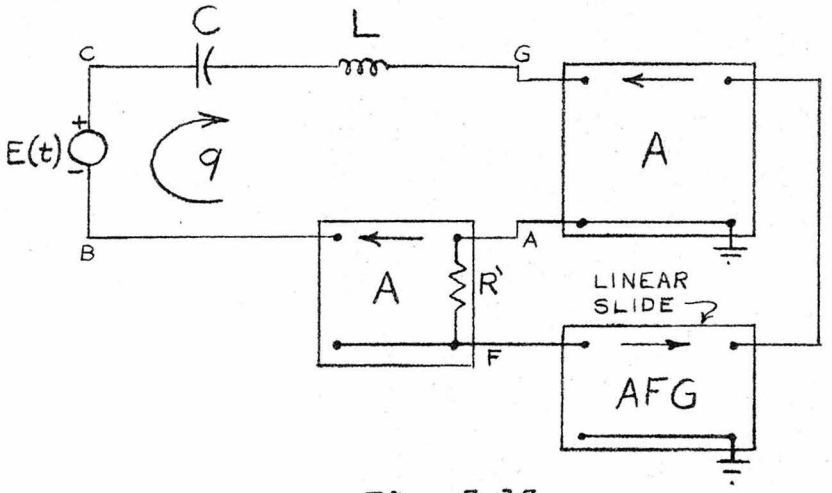

Fig. 3.13

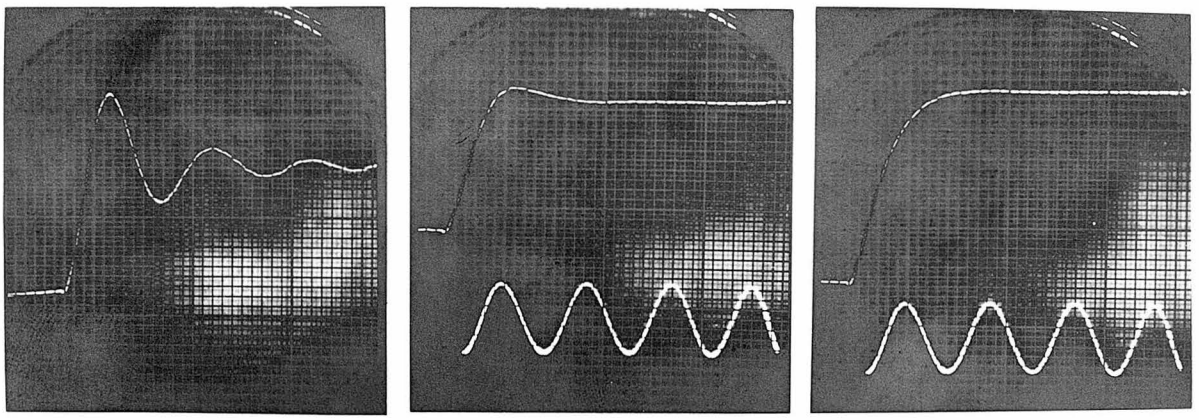

$\zeta = 0.2$ (a)　　$\zeta = 0.6$ (b)　　$\zeta = 1.0$ (c)

FIG. 3.14　RESPONSE, LINEAR SPRING

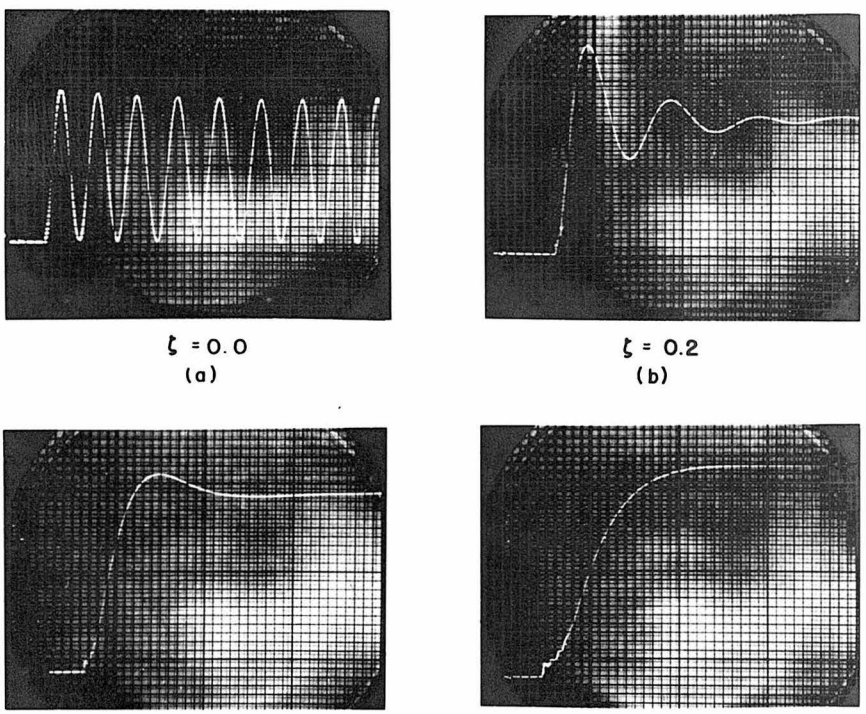

$\zeta = 0.0$ (a)　　$\zeta = 0.2$ (b)

$\zeta = 0.6$ (c)　　$\zeta = 1.0$ (d)

FIG. 3.15　RESPONSE, LINEAR DAMPING

highly damped transient in this case of the arbitrary function generator being used as a linear damper. This is in contrast to the previous section where the parasitic oscillation accompanied the low damping case. However, in either case, the parasitic oscillation appears when there is a relatively large output voltage from the feedback loop applied between busses A and G.

5. The accuracy of the arbitrary function generator

The accuracy of the experimental solutions of nonlinear differential equations naturally depends quite significantly upon the ability of the arbitrary function generator to produce accurately an output voltage that is the required function of the input voltage. The only nonlinear slide used in this experimental work was one of the curve $y = x^3$. It was produced by photographing a "mask" drawn accurately on a piece of cardboard with 1 ft. x 2 ft. dimensions.

The types of errors that are inherent in an arbitrary function generator of this type are discussed at length in a thesis by Buchholz. (7) Therefore, the treatment of errors that is given here will be somewhat abbreviated. The most important types are:

a. Parallax

Since the mask is not in contact with the phosphor surface of the oscilloscope tube, the actual beam position will be affected by parallax. If the screen were flat, the effect of parallax would be, for the most part, just a

change of scale. However, the curvature of the screen causes an increased parallax effect, particularly near its circumference.

In order to minimize errors due to parallax, the working area is restricted to the central portion (1" x 2") of the screen. A 3GP15A tube is used.

b. Cathode ray tube distortion

The output voltage will be inaccurate if the deflection sensitivity is not a constant throughout the working area of the screen. This results from the fact that the output voltage is directly proportional to the deflection voltage.

c. Maximum spot velocity, $\dot{y}$

This effect limits the frequency response of the generator and, therefore, is most noticeable for either high sweep rates or for mask patterns with steep slopes. The main cause of the limited spot velocity, $\dot{y}$, is the time constant of the phototube circuit. Also, the maximum spot velocity going in the direction of increasing y is approximately twice as fast as the maximum velocity going in the opposite direction. The effect of a limited spot velocity is similar to the attenuation and phase shift of a low pass filter. For the slides used in this work (linear and cubic), the limited spot velocity caused no trouble since the driving frequencies were quite low.

d. Halo effect

If the mask has sharp "peaks" or "valleys", the spot will tend to avoid them. This is due to the finite spot

dimensions. For example, if equilibrium occurs with half the spot exposed, the center of the spot will follow a straight edge of the mask. However, the center will lie below the top of a "peak" when half the spot is exposed. Similarly, the center of the spot will lie above the bottom of a "valley".

e. Steady state error

There is an error that is proportional to the distance y from the center of the pattern and inversely proportional to the loop gain. Since this model of the arbitrary function generator uses a voltage clipper to keep the spot from leaving the screen, a higher loop gain can be used and the accuracy is thereby improved.

f. Dead spots

If a point on the screen undergoes continued bombardment by the electron beam, it will eventually fatigue and its output of light will decrease. This is most likely to occur at a point corresponding to the center of the pattern, i.e., the point at which the beam rests when there is no input to the arbitrary function generator. Due to the decreased light intensity coming from this point, the beam will tend to avoid it, and the output voltage will act as though the pattern has a "bump" on it. If a dead spot appears on the screen, it can usually be avoided by moving the slide slightly.

g. Errors of adjustment

Of course, serious errors can occur in the AFG output

due to lack of proper adjustment. For example, the bias voltage on the horizontal deflection plates must be such that the spot rests at $x = 0$ for no input voltage. The dc level of the output must be such that there is no output voltage when the spot is at $y = 0$. Also, the spot focus and intensity should be adjusted to give optimum performance.

Care should be taken to insure that the x and y axes of the slide are parallel to the corresponding axes of the cathode ray tube. A small angular displacement of the slide relative to the tube will have the effect of adding a linear term to the function represented on the slide.

Actually, none of the above possibilities for error proved to be serious. Fig. 3.16 shows that the output voltage was remarkably accurate (for the case of a cubic slide) until the input was reduced to the noise level (0.02 volts rms input). The noise is due partly to pickup and partly to slight imperfections in the screen in the neighborhood of the origin.

ACCURACY OF ARBITRARY FUNCTION GENERATOR

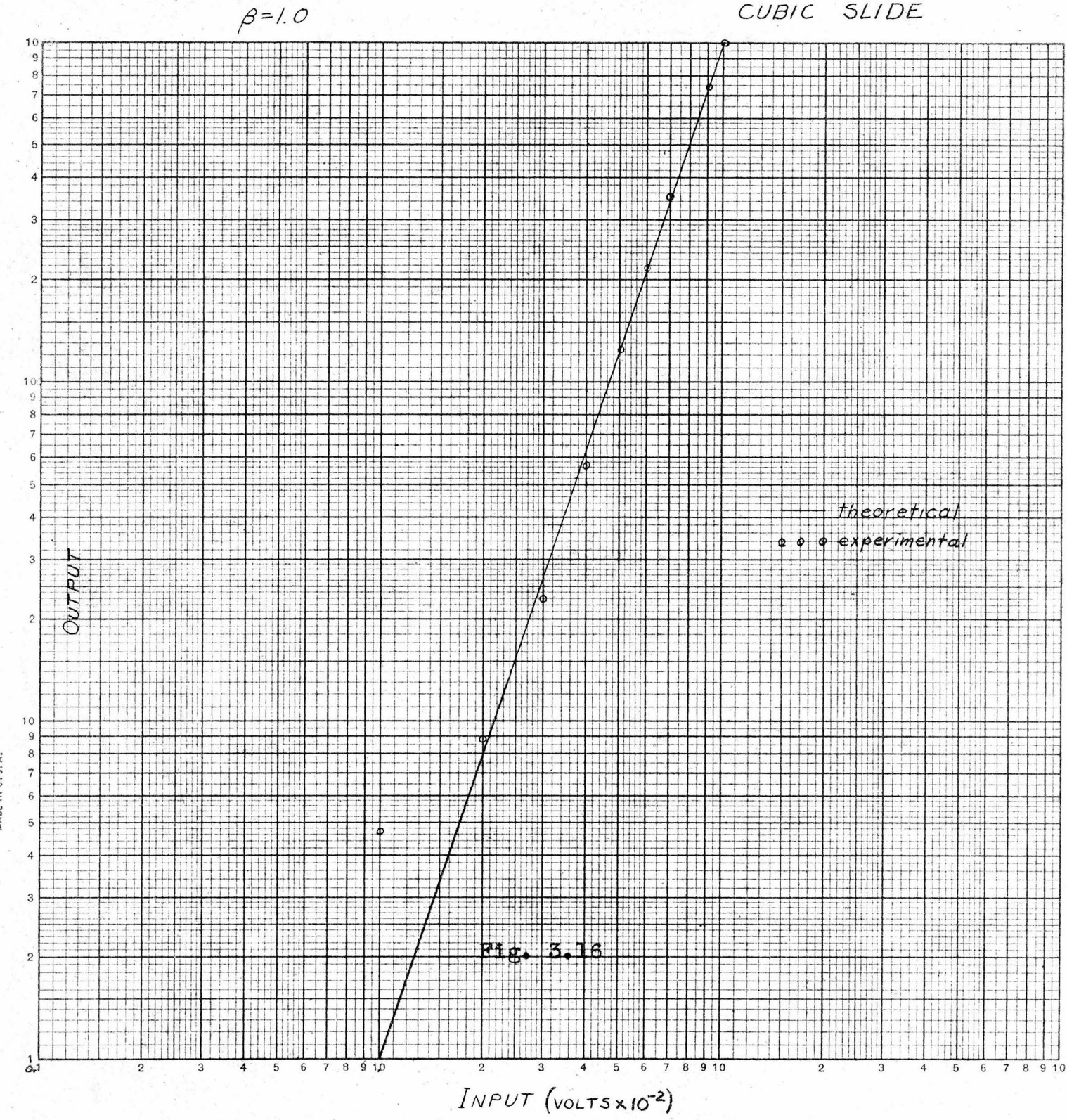

Fig. 3.16

PART IV

SYSTEMS WITH A NONLINEAR RESTORING FORCE

1. Duffing's equation

The differential equation describing the forced oscillations of a system with one degree of freedom and in which the restoring force is a nonlinear function of position is as follows:

$$m\ddot{x} + c\dot{x} + f(x) = F \cos \omega t \tag{19}$$

In the case of a simple mechanical system the nonlinear term corresponds to a spring force.

For the particular case where $f(x)$ is of the form

$$f(x) = \alpha x + \beta x^3 \tag{20}$$

the equation is known as Duffing's equation. Duffing's equation as applied to an electrical series circuit takes the form

$$L\ddot{q} + R\dot{q} + \frac{q}{C} + Aq^3 = E \cos \omega t \tag{21}$$

Dividing through by L we obtain

$$\ddot{q} + \frac{R}{L}\dot{q} + \frac{q}{LC} + \frac{A}{L}q^3 = \frac{E}{L} \cos \omega t \tag{22}$$

Making the substitution

$$\tau = \frac{t}{\sqrt{LC}} \tag{23}$$

and denoting $\frac{dq}{d\tau}$ by q', $\frac{d^2q}{d\tau^2}$ by q", etc. equation (22) becomes

$$\frac{q''}{LC}+\frac{R}{L\sqrt{LC}}q'+\frac{q}{LC}+\frac{A}{L}q^3 = \frac{E}{L}\cos\omega\sqrt{LC}\,\tau$$

or

(24) $$q''+\frac{R}{\sqrt{\frac{L}{C}}}q'+q+ACq^3 = EC\cos\omega\sqrt{LC}\,\tau$$

Now let

(25) $$u = \frac{q}{EC}$$

(26) $$\zeta = \frac{R}{2\sqrt{\frac{L}{C}}}$$

(27) $$\gamma = E^2C^3A$$

(28) $$\beta = \omega\sqrt{LC}$$

and equation (24) becomes

(29) $$u''+2\zeta u'+u(1+\gamma u^2) = \cos\beta\tau$$

This is Duffing's equation in dimensionless form.

2. Electrical circuit with nonlinear restoring force

The electrical circuit used in analyzing Duffing's equation is shown in Fig. 4.01.

The computer signal generator is connected between busses B and C. The voltage BC is about 2 volts rms.

The linear term in u is represented by the 0.1 μf capacitor. The voltage corresponding to the cubic term appears across AG. A cubic slide ($y = x^3$) is placed in the arbitrary function generator. The input voltage AF is taken from across a 2.4 μf capacitor. (The 4 μf, 6 μf series arrangement was used because the minimum gain of the amplifier between A and B is greater than unity. Using the voltage divider, the gain of the amplifier is adjusted to give minimum voltage across AB.)

The desired value of γ is obtained by adjusting the loop gain, either by varying the gain of the amplifier between A and G or adjusting the input or output attenuators of the arbitrary function generator. Now

$$(30) \qquad \gamma = \frac{1}{u^2_{max}} \frac{\text{peak voltage across nonlinear capacitor}}{\text{peak voltage across linear capacitor}}$$

$$= \frac{1}{u^2_{max}} \frac{V_{AG}}{V_{DG}}$$

where

$$(31) \qquad u_{max} = \frac{\frac{q_{max}}{C}}{E} = \frac{V_{DG}}{V_{BC}} \quad \text{(peak voltages)}$$

Another expression is

$$(32) \qquad \gamma = \frac{1}{u^3_{max}} \frac{V_{AG}}{V_{BC}}$$

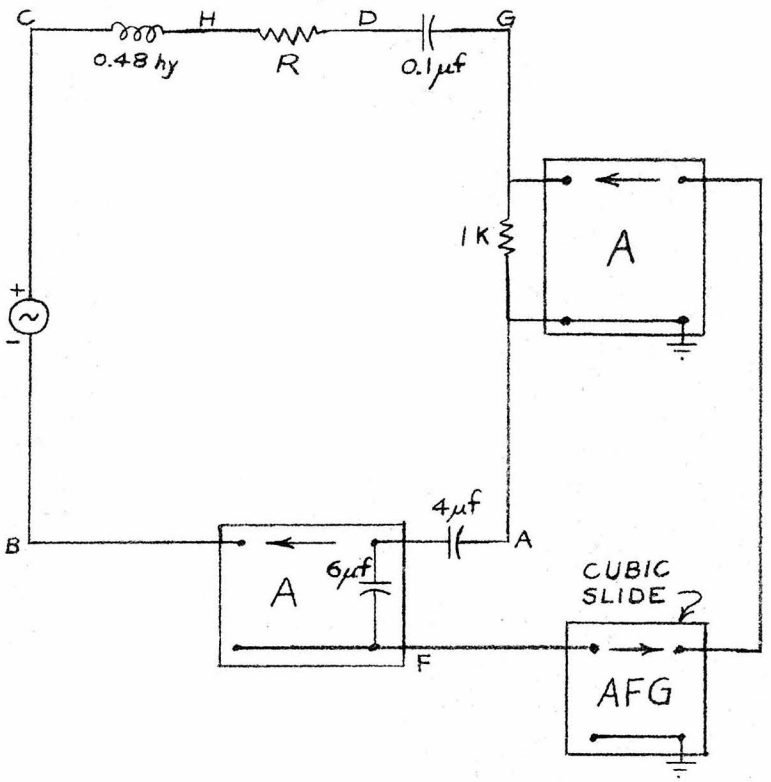

Fig. 4.01

The resistor R is set to give the correct value of damping. Allowance is made for changes of inductor resistance with frequency.

In taking this data, a filter is used on the input to the amplifier between A and G. The actual resonant frequency for the case $\zeta = 0$, $\gamma = 0$ is 719 cps.

3. Results

The response curves for $\gamma = 0.40$ are shown in Figs. 4.02 and 4.03. These curves are plots of the steady state amplitude G vs. the frequency β for Duffing's equation in dimensionless form.* By comparing these curves with those for the linear case, it may be seen that the response curves are "bent" to the right, causing the maximum amplitude to occur at a higher frequency. The most striking effect for low values of damping is that discontinuities or "jumps" occur in the amplitude characteristic. An additional result of the nonlinearity is that the jumps in each direction do not occur at the same frequency, thereby giving the curves a form resembling a hysteresis loop. In the low energy range, the system acts quite linearly, both in amplitude and waveform. However, the cubic term becomes important at high energies and the voltage AG (corresponding

---

* The "amplitude" of the periodic response of a nonlinear system is the peak amplitude. Since the nonlinearities are symmetrical about the system equilibrium, the peak amplitudes in positive and negative directions will be equal.

to the force of the cubic spring) is of the same order of magnitude as the voltage DG (linear spring force). For example, if $\gamma = 0.4$, the forces of the linear and cubic springs are equal for energies corresponding to G = 1.6. Even for values of ζ where no jump occurs, there is a noticeable shift in the frequency at which the maximum vibration amplitude occurs.

For the case of negative γ (See Figs. 4.04 and 4.05.) the response curves are bent to the left. Similar jump phenomena occur. Negative values of γ cause one new characteristic of the oscillation; namely, a tendency toward instability. Unless γ is kept quite small, the force of the cubic spring will become larger than the restoring force of the linear spring and the displacement u will go off to infinity. This tendency is most pronounced for low values of ζ and for values of β giving large G. As an example, if $\gamma = -0.02$, instability will occur for $G > 7$.

It would seem that, theoretically, instability would occur only for the case where the curves bend to the left far enough to intersect the $\beta = 0$ axis. Experimental results indicate that instability occurs at higher frequencies, however. Perhaps the difference is due to the destabilizing influences of noise, ripple, etc.

Fig. 4.06 (a) shows the steady state response for the case $\gamma = 0.4$, $\zeta = 0.2$. The oscillation is approximately sinusoidal. Thus, the nonlinearity seems to affect the response curves primarily rather than the waveform. The

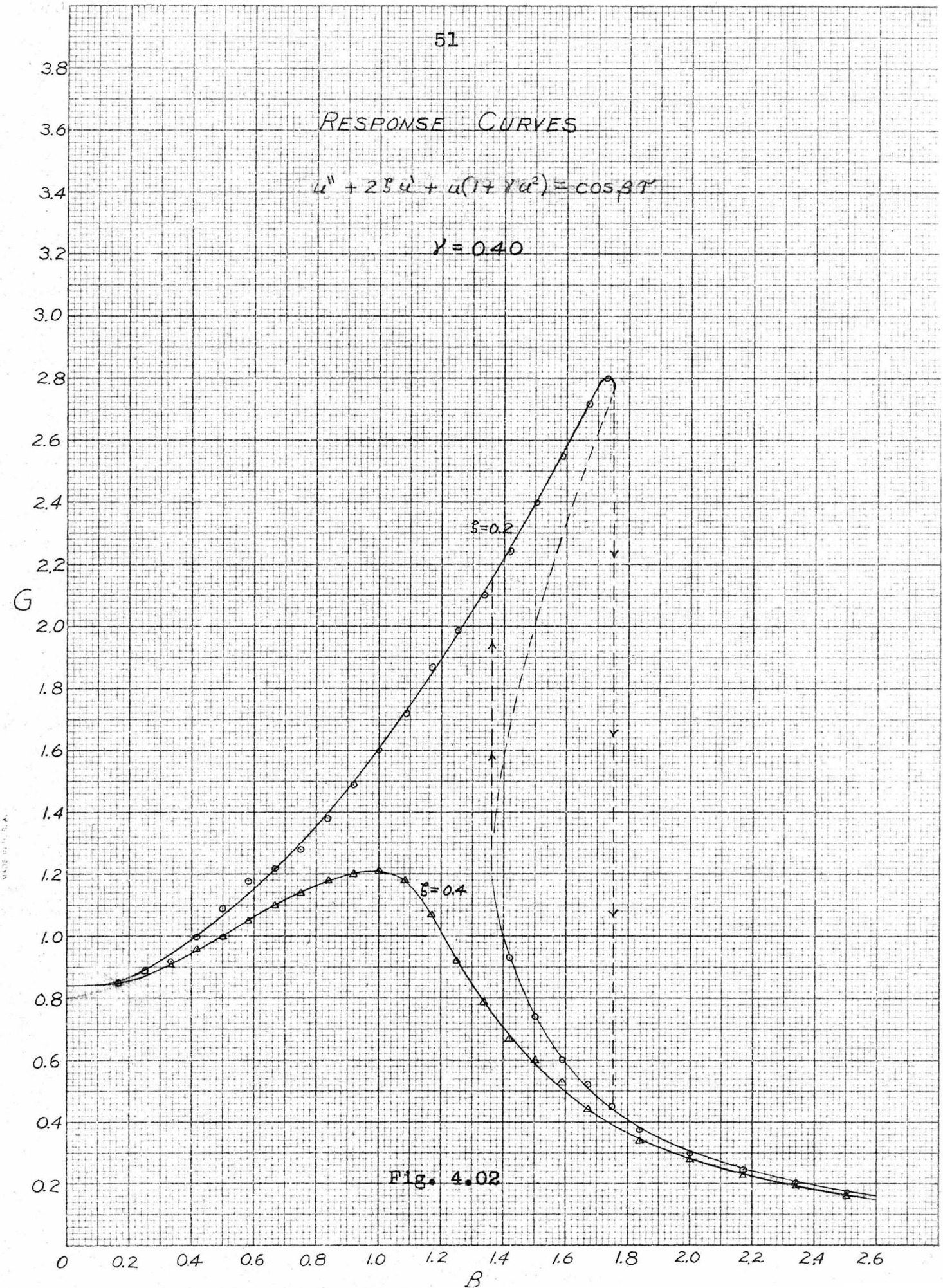

Fig. 4.02

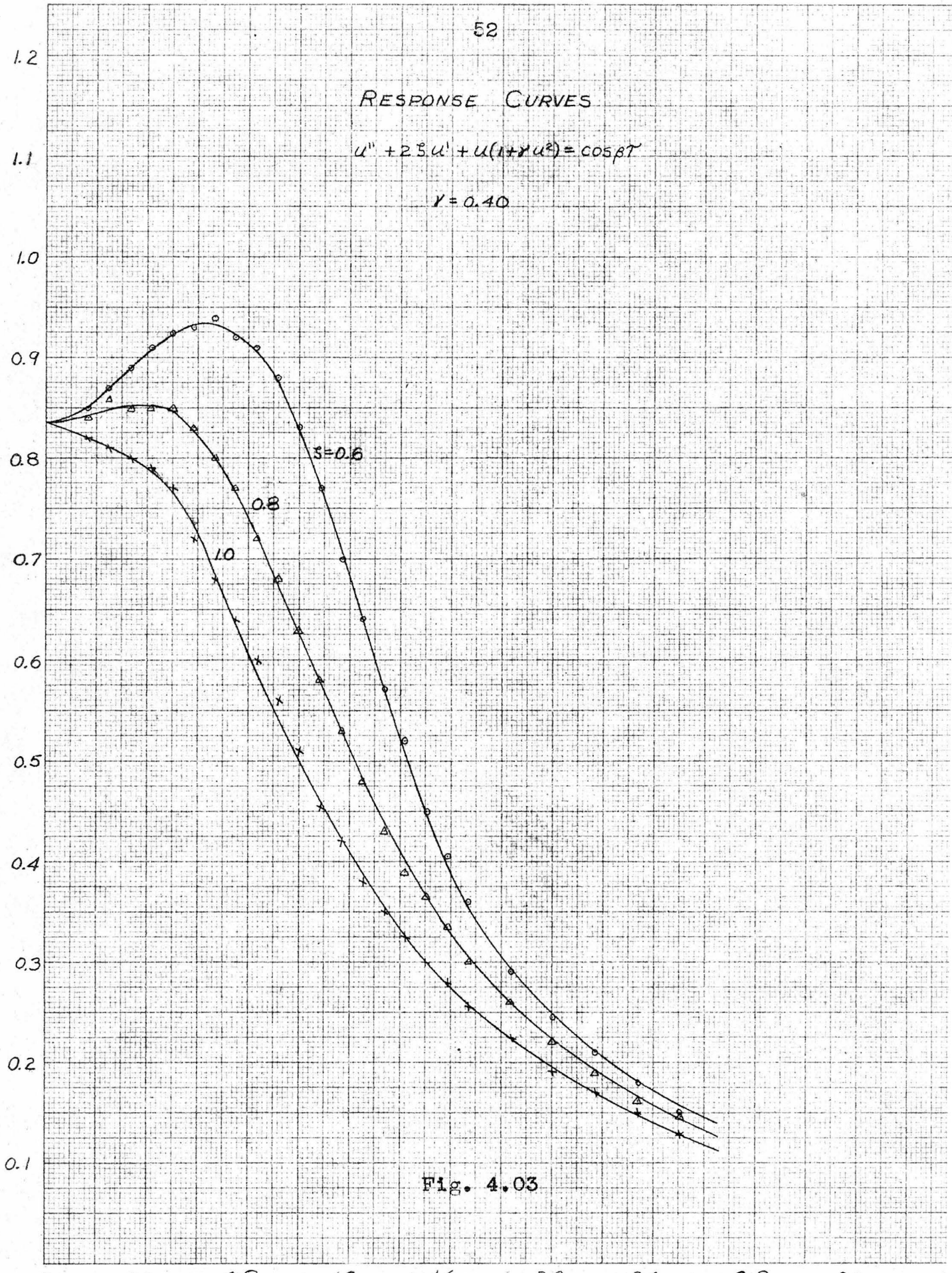

Fig. 4.03

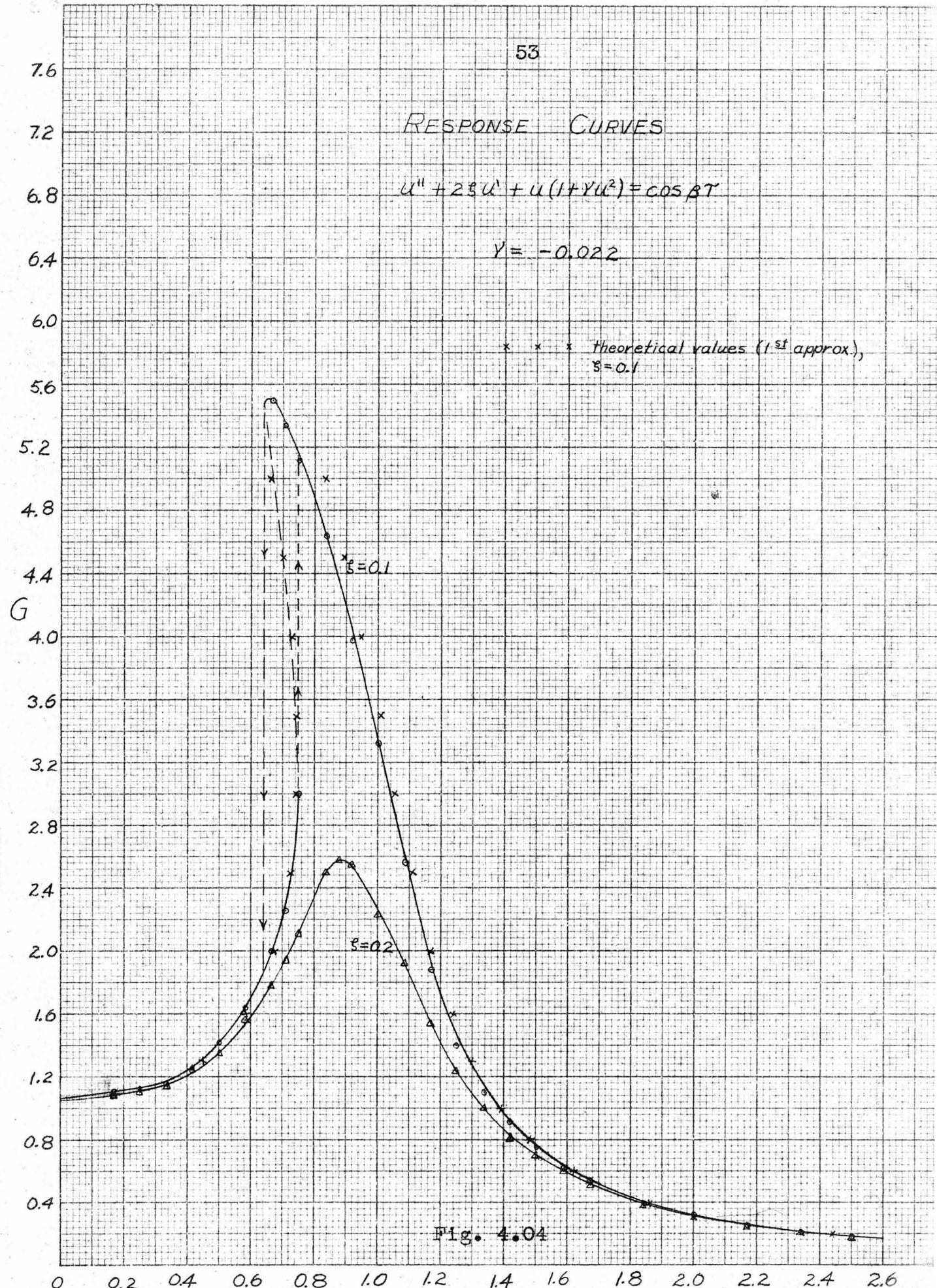

Fig. 4.04

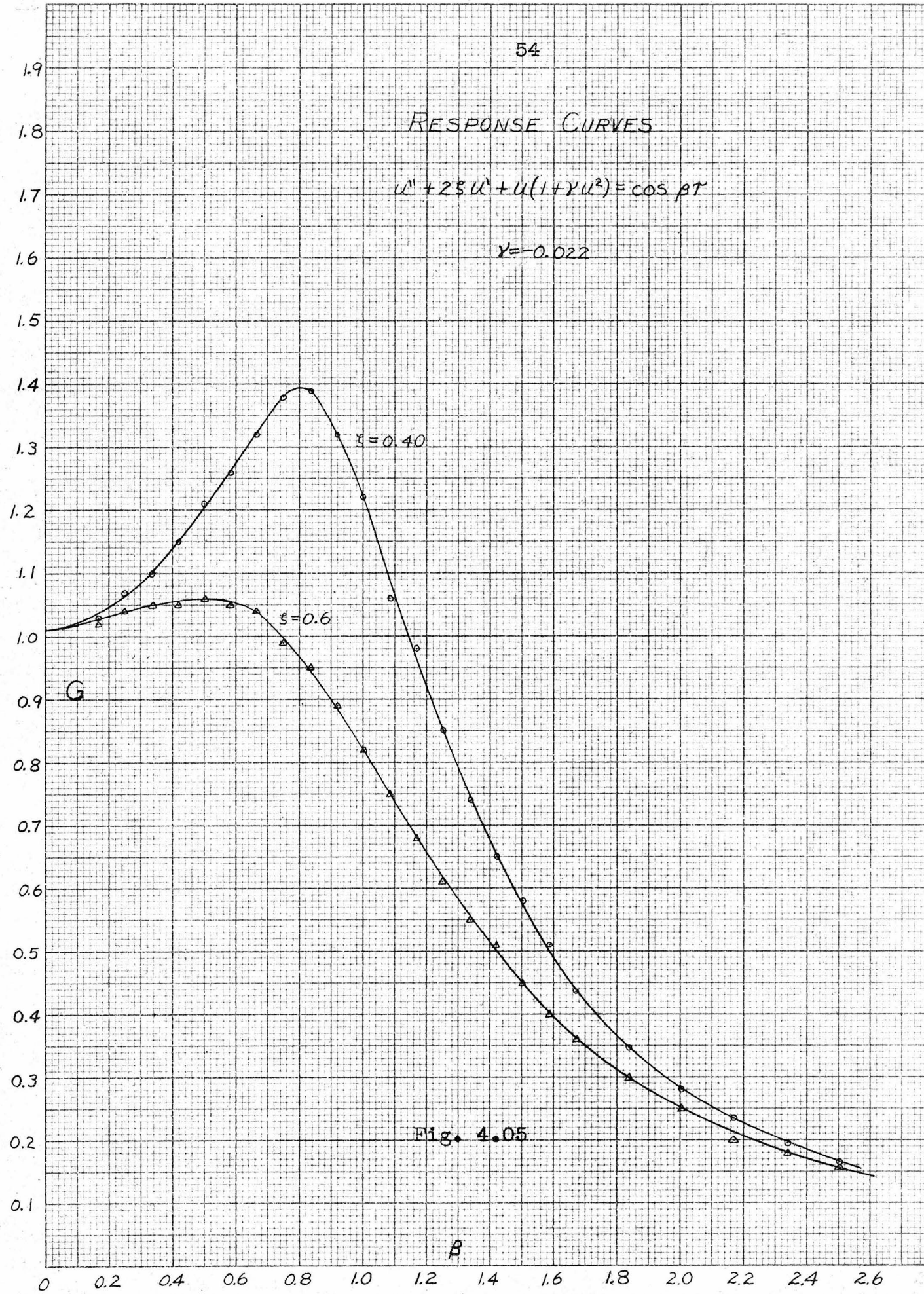

Fig. 4.05

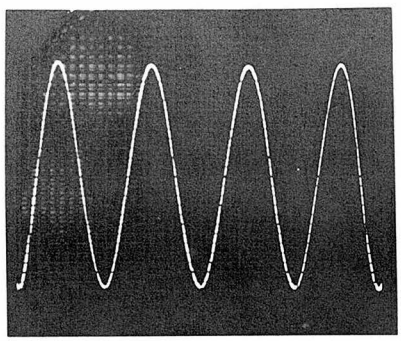

$\zeta = 0.2$
$\gamma = 0.4$
(a)

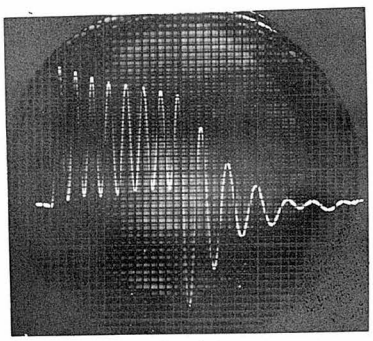

$\zeta = 0.1$
$\gamma = 0.4$
(b)

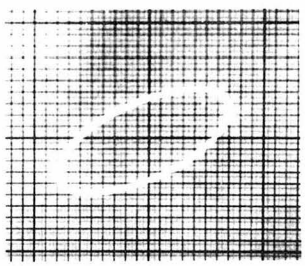

$\zeta = 0.1$
$\gamma = -0.022$
(c)

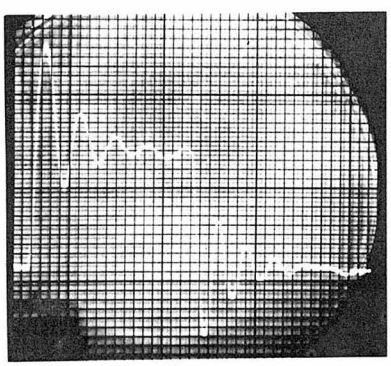

$\zeta = 0.1$
$\gamma = -0.022$
(d)

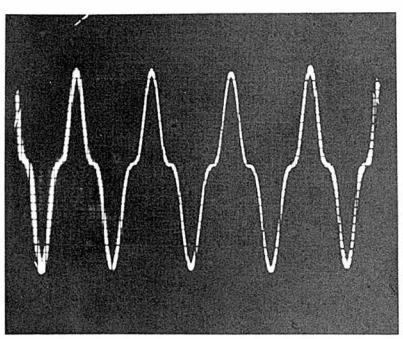

$\zeta = 0.1$
$\gamma = -0.022$
(e)

FIG. 4.06 NONLINEAR SPRING

transient response to a square pulse (amplitude = 2.1) is shown in Fig. 4.06 (b). Note that the oscillation frequency is higher during the pulse. This is because the spring constant is larger due to the increased influence of the cubic term at large displacements. The oscillations about equilibrium are of low enough amplitude that the departure from linearity is not marked.

Note also that the damping appears to be larger for vibrations about equilibrium, i.e., the amplitude of the oscillations seems to diminish more rapidly. Considered on an energy basis, however, this is seen not to be the case. The rate of energy dissipation is actually larger during the pulse (for a given peak to peak amplitude of oscillation) because of the larger average velocity. The cubic term in the spring force expression causes the potential energy to have a term proportional to the fourth power of the displacement. Therefore, relatively large energy changes may occur without a marked change in the amplitude of oscillation. This gives a "hard" spring the effect of limiting oscillation amplitudes.

Fig. 4.06 (c) shows a Lissajous figure of displacement vs. driving force for the case of a "soft" spring ($\gamma = -0.022$) with $\zeta = 0.1$. The elliptical form shows that in this case also the oscillation is approximately sinusoidal.

Fig. 4.06 (d) shows the response to a pulse of amplitude 2.1 for the case $\gamma = -0.022$. In this case, the frequency is lower during the pulse, while the apparent damping

is larger. This is in contrast to the case of positive γ and can be explained by reversing the effects mentioned in that discussion.

The spring force is shown as a function of time in Fig. 4.06 (e). The frequency in this case is $\beta = 1.0$, and the amplitude of the spring force is 2.5.

4. Approximate solution

In order to get some idea of the accuracy of the analog computer in the analysis of nonlinear systems of this sort, we will check the case $\gamma = -0.022$, $\zeta = 0.1$ against an approximate solution. We will follow the method used by Duffing (9), applying it to the case where damping is present.

There will be a difference in phase between the driving force and the displacement. Therefore, let us put the differential equation in the form

$$u'' + 2\zeta u' + u(1+\gamma u^2) = \cos(\beta\tau + \phi) \tag{33}$$

$$= \cos\phi \cos\beta\tau - \sin\phi \sin\beta\tau$$

and assume a zero order approximation

$$u_0 = A \cos\beta\tau \tag{34}$$

Then ϕ can be obtained as well as an equation for determining β as a function of A.

Substituting equation (34) into equation (33) and noting that

$$\cos^3\beta\tau = \tfrac{3}{4}\cos\beta\tau + \tfrac{1}{4}\cos 3\beta\tau$$

we obtain

$$(35)\qquad (A - A\beta^2 + \tfrac{3}{4}\gamma A^3)\cos\beta\tau - 2\zeta\beta A\sin\beta\tau + \frac{\gamma A^3}{4}\cos 3\beta\tau$$

$$= \cos\phi\cos\beta\tau - \sin\phi\sin\beta\tau$$

Now we neglect the term $(\frac{\gamma A^3}{4}\cos 3\beta\tau)$ and set the coefficients of $\cos\beta\tau$ and $\sin\beta\tau$ equal. There results

$$(36)\qquad A - A\beta^2 + \tfrac{3}{4}\gamma A^3 = \cos\phi$$

$$(37)\qquad -2\zeta\beta A = \sin\phi$$

but

$$\sin^2\phi + \cos^2\phi = 1$$

or

$$(38)\quad \beta^4 + (4\zeta^2 - 3/2\gamma A^2 - 2)\beta^2 + (9/16\gamma^2 A^4 + 3/2\gamma A^2 + 1 - \frac{1}{A^2}) = 0$$

giving β^2 as a function of A.

$$(39)\quad \beta^2 = -(2\zeta^2 - \tfrac{3}{4}\gamma A^2 - 1) \pm \left[4\zeta^2(\zeta^2 - \tfrac{3}{4}\gamma A^2 - 1) + \frac{1}{A^2}\right]^{\frac{1}{2}}$$

The plot of the amplitude vs. frequency calculated from equation (39) for the case $\zeta = 0.1$ is shown in Fig. 4.04. The agreement of experimental and calculated values is quite good except near the peak where there is a wider spread in the values of β for a given G.

There seems to be some reason for believing that the experimental values are actually more accurate than the first order calculations for large amplitudes. The neglected term in the calculations, namely, $\frac{\gamma A^3}{4}\cos 3\beta T$, is proportional to the cube of the amplitude and thus the error would be expected to be much larger near the peak of the curve.

PART V

SYSTEMS WITH NONLINEAR DAMPING FORCE

In this consideration of nonlinear damping forces we shall treat both forced and free oscillations. In the latter case the specific system will be that covered by van der Pol's equation.

1. Forced Oscillations

a. Equation for cubic damping term

The mechanical equation for forced oscillations with nonlinear damping is

$$m\ddot{x} + g(\dot{x}) + kx = F\cos\omega t \tag{40}$$

We shall consider the particular case where

$$g(\dot{x}) = c\dot{x} + e\dot{x}^3 \tag{41}$$

giving the mechanical equation

$$m\ddot{x} + c\dot{x} + e\dot{x}^3 + kx = F\cos\omega t \tag{42}$$

Its electrical analog is

$$L\ddot{q} + R\dot{q} + h\dot{q}^3 + \frac{q}{C} = E\cos\omega t \tag{43}$$

The dimensionless form of this equation is

$$u'' + 2\zeta u' + \mu u'^3 + u = \cos\beta\tau \tag{44}$$

where

(45) $$u = \frac{q}{EC}$$

(46) $$\tau = \frac{t}{\sqrt{LC}}$$

(47) $$\zeta = \frac{R}{2\sqrt{\frac{L}{C}}}$$

(48) $$\mu = \frac{E^2 h}{\left(\frac{L}{C}\right)^{3/2}}$$

b. Electrical circuit

The electrical circuit used to represent this equation is Fig. 5.01. ζ is set to the correct value by adjusting R. The term $\mu u'^3$ appears as the voltage AG. A cubic slide is used in the arbitrary function generator.

The coefficient μ is set to the desired value by using the equation

(49) $$\mu = \frac{1}{u'^3} \frac{V_{AG}}{V_{BC}}$$

where

(50) $$u' = \frac{1}{2\zeta} \frac{V_{DH(corrected)}}{V_{BC}}$$

The corrected voltage is obtained by multiplying the actual voltage V_{DH} by the ratio $\frac{\text{total system resistance}}{R}$. Note that the actual value of the resistor between D and H is smaller

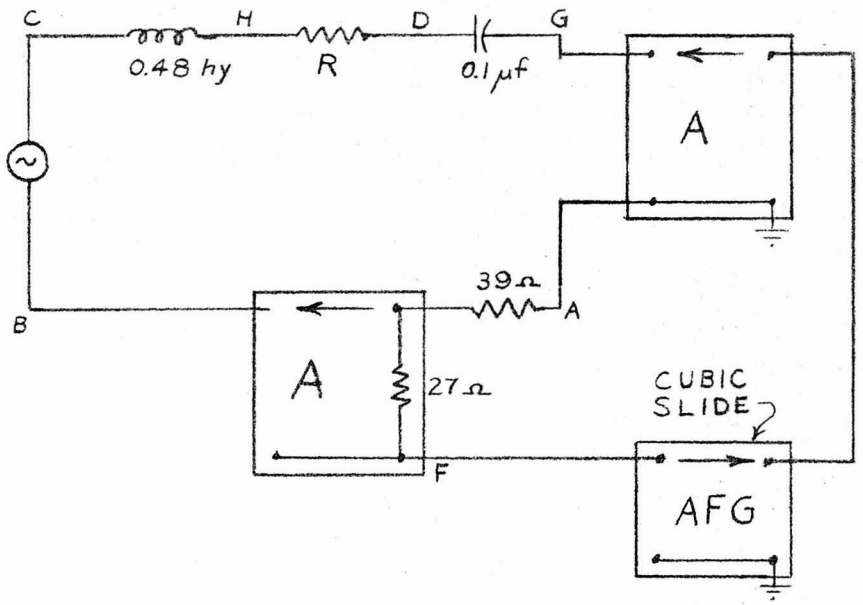

Fig. 5.01

than $2\zeta\sqrt{\frac{L}{C}}$ since the other elements, notably the inductor, have a resistive component which cannot be neglected.

c. Results

The response curves for the case $\mu = 1$ are shown in Figs. 5.02 and 5.03. Comparing these curves with the corresponding linear damping curves (Figs. 3.01 and 3.02) several differences may be noted.

First, the cubic damping causes lower vibration amplitudes. This effect is most noticeable for small ζ. For example, the maximum amplitude of the response curve for cubic damping with $\zeta = 0$ is roughly equal to that for linear damping with $\zeta = 0.4$.

Another effect of the cubic damping is the lowering of the frequency corresponding to maximum amplitude. For example, with $\zeta = 0$, the maximum amplitude occurs at $\beta = 0.66$ compared with $\beta = 1.0$ for the linear case. Thus, qualitatively speaking, the cubic damping term presents a strong bias against large velocities. Now since the velocity, for a given amplitude, is directly proportional to the frequency β, the cubic damping term causes the maximum amplitude to occur at a somewhat lower frequency.

For negative μ the peak amplitudes are higher, particularly for small ζ. (See Fig. 5.04.) In fact, μ must be kept small in order that the system remain stable with u finite. For the case $\mu = -0.02$, the peak amplitudes in the response curve occur at slightly higher frequencies and it is assumed that this effect would be more pronounced for

more negative values of μ.

Figs. 5.05 (a), (b) and (c) show the steady state displacement, velocity and acceleration for the case of $\mu = 1.0$, $\zeta = 0.1$, $\beta = 1.0$. It can be seen that there are significant changes from the sinusoidal waveforms that would occur for $\mu = 0$.

Figs. 5.05 (d) and (e) show the displacement and velocity due to a step function of magnitude 0.7. Note that the cubic damping discriminates against high velocities. This can be seen by the very high damping on the first oscillation of the velocity curve.

Figs. 5.05 (f), (g) and (h) show the steady state displacement, velocity and acceleration for the case where all the damping is cubic, i.e., $\zeta = 0$. They are seen to be quite similar to the corresponding case of $\zeta = 0.1$ except that the departure from a sinusoidal waveform is even greater.

Fig. 5.05 (i) shows the displacement for the case of negative cubic damping. In this case the waveform is essentially sinusoidal. Greater deviations could be obtained with slightly more negative values of μ. However, as was pointed out previously, the system becomes unstable (the displacement goes to infinity) for much more negative μ.

d. Analytic approach

Consider the equation

$$u'' + 2\zeta u' + \mu u'^3 + u = \cos(\beta\tau + \phi) \tag{51}$$

where the phase angle ϕ has been added to the forcing

RESPONSE CURVES — CUBIC DAMPING

$$u'' + 2\zeta u' + \mu u^3 + u = \cos \beta\tau$$

$$\mu = 1$$

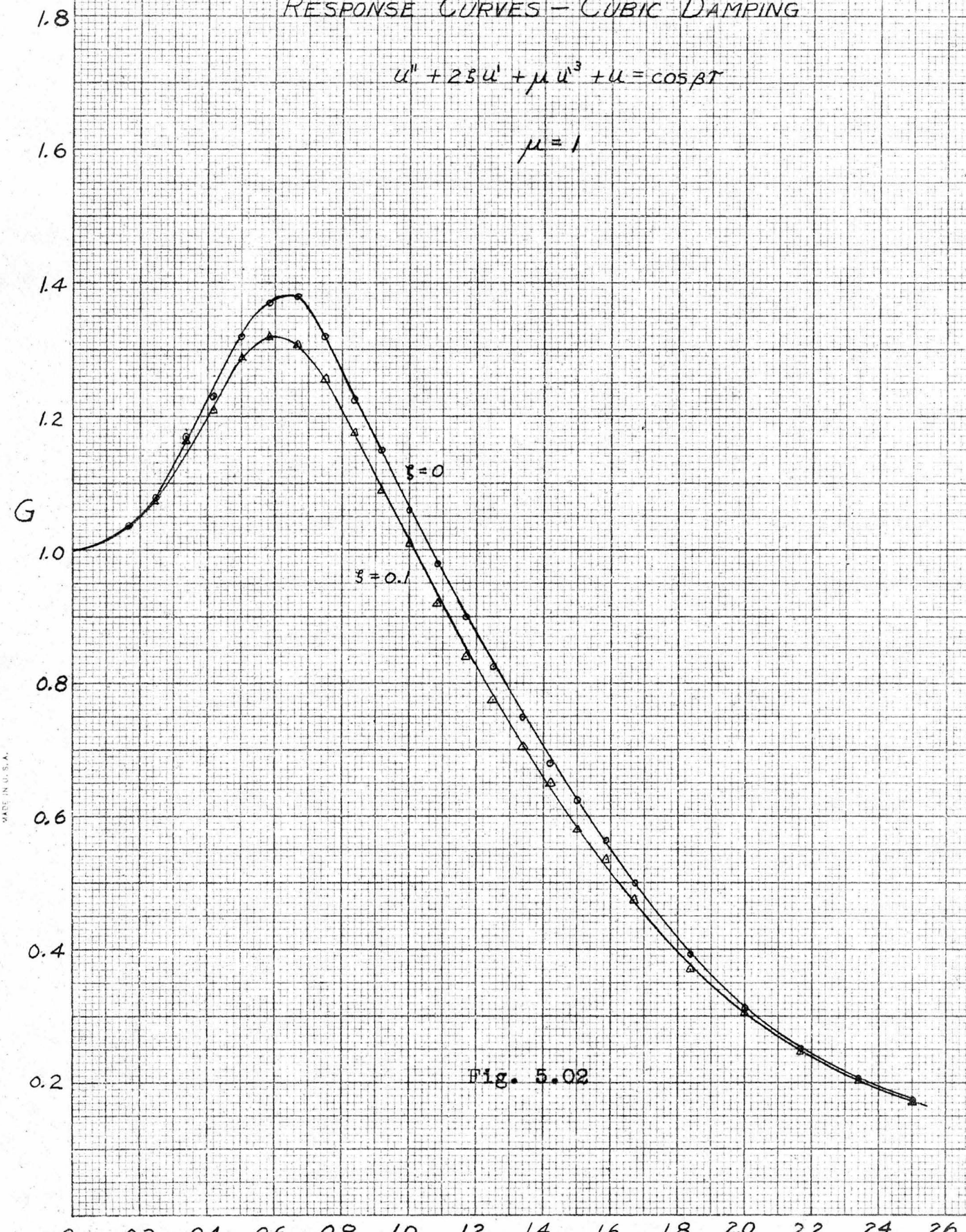

Fig. 5.02

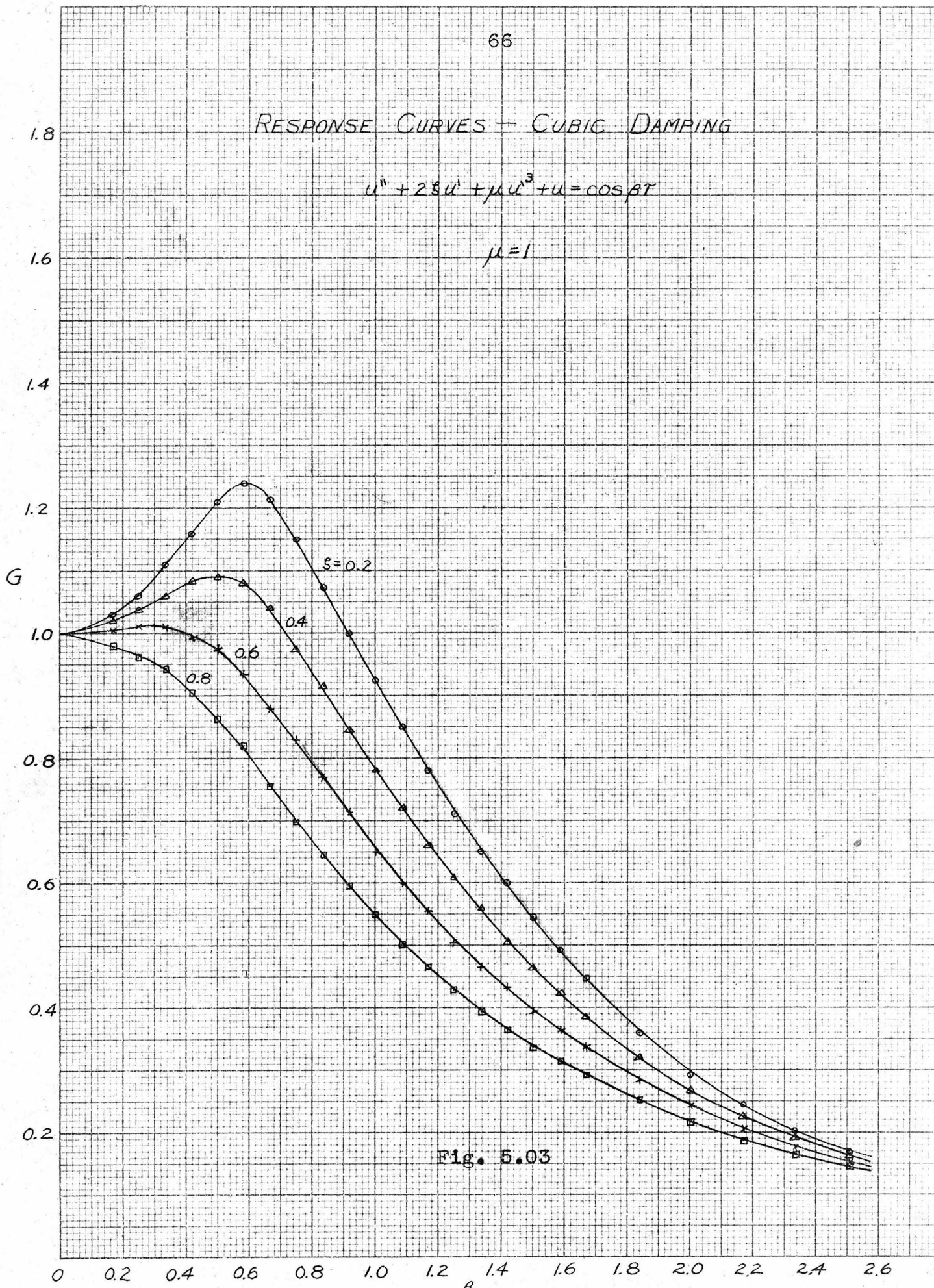

Fig. 5.03

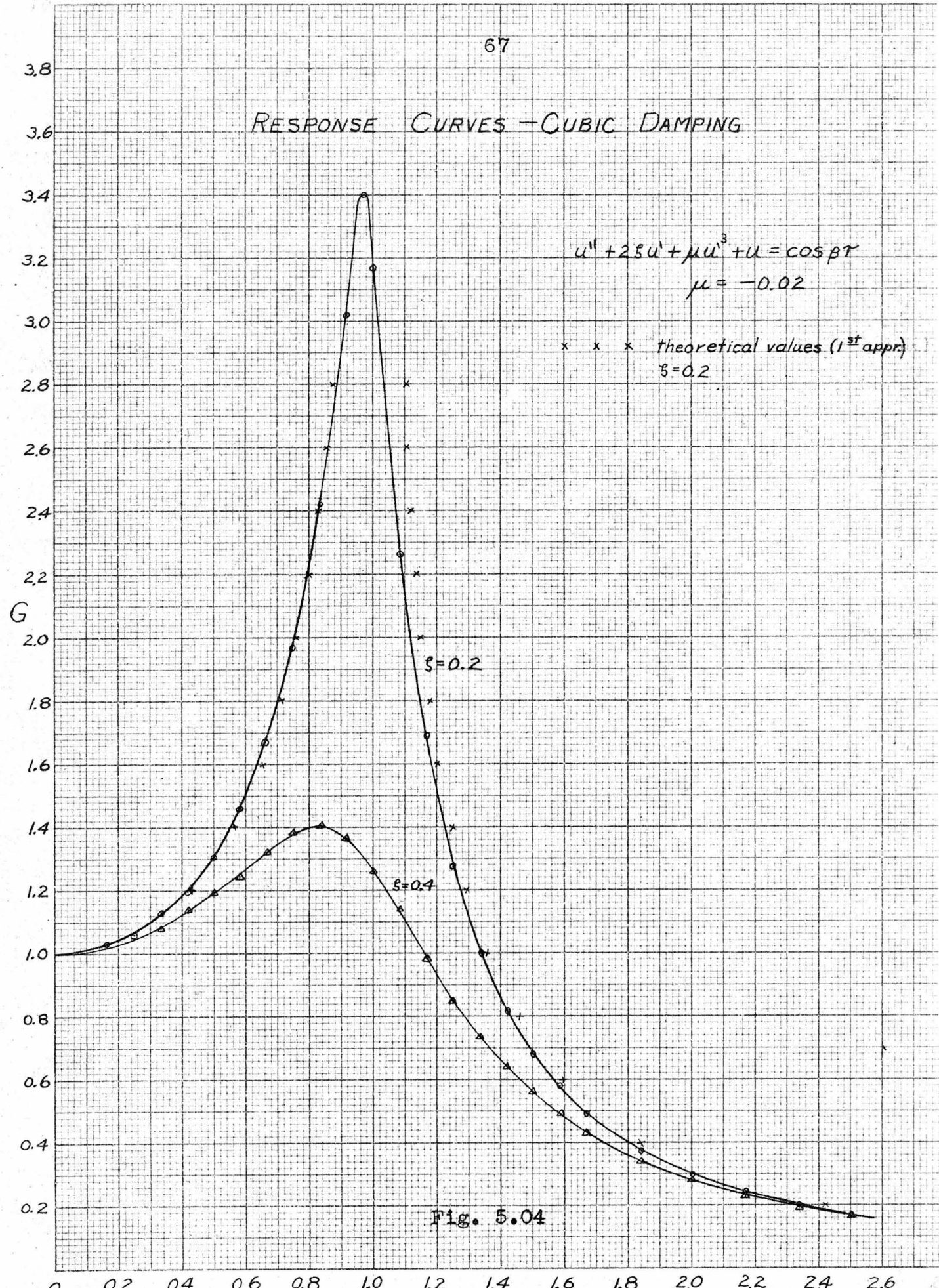

Fig. 5.04

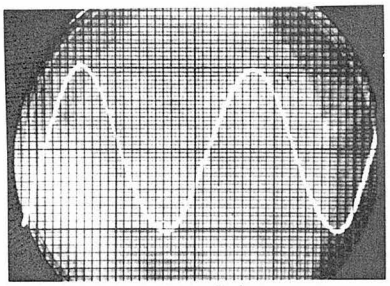

$\zeta = 0.1$
$\mu = 1.0$
$\beta = 1.0$
(a)

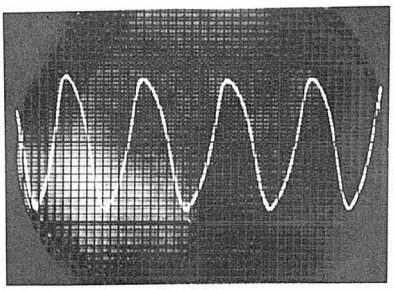

$\zeta = 0.1$
$\mu = 1.0$
$\beta = 1.0$
(b)

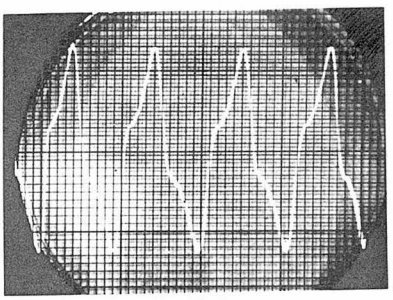

$\zeta = 0.1$
$\mu = 1.0$
$\beta = 1.0$
(c)

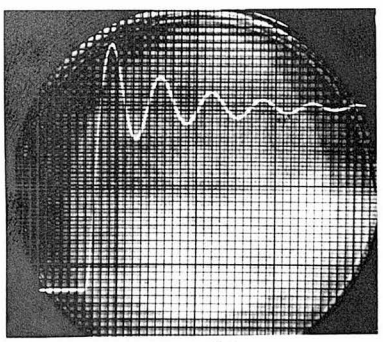

$\zeta = 0.1$
$\mu = 1.0$
(d)

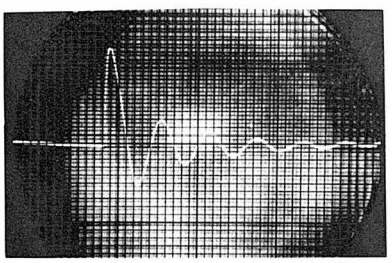

$\zeta = 0.1$
$\mu = 1.0$
(e)

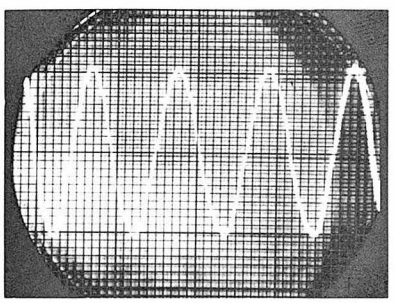

$\zeta = 0.1$
$\mu = 1.0$
$\beta = 1.0$
(f)

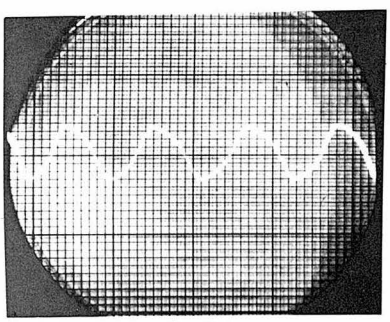

$\zeta = 0.1$
$\mu = 1.0$
$\beta = 1.0$
(g)

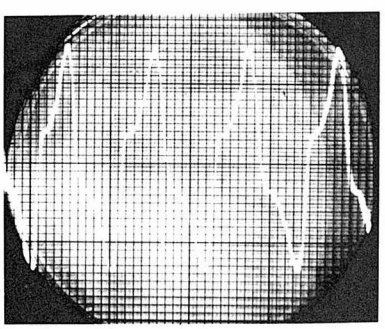

$\zeta = 0.1$
$\mu = 1.0$
$\beta = 1.0$
(h)

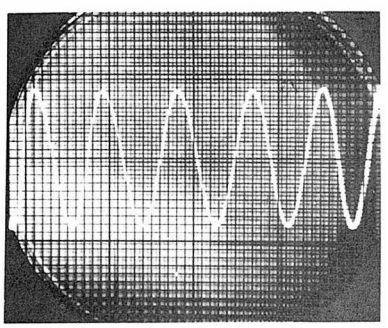

$\zeta = 0.2$
$\mu = -0.02$
$\beta = 1.0$
(i)

FIG. 5.05 NONLINEAR DAMPING

function in order that the zero order approximation need not include a phase angle.

Now assume the approximate solution

$$u_o = A\cos\beta\tau$$

Substituting into equation (51) and expanding the right side we obtain

$$(52)\quad -A\beta^2\cos\beta\tau - 2\zeta A\beta\sin\beta\tau - \mu A^3\beta^3\sin^3\beta\tau + A\cos\beta\tau = \cos\phi\cos\beta\tau - \sin\phi\sin\beta\tau$$

Now

$$\sin^3\beta\tau = -\frac{\sin 3\beta\tau}{4} + \frac{3}{4}\sin\beta\tau$$

If we neglect the term containing $\sin 3\beta\tau$, equation (52) becomes

$$(53)\quad A(1-\beta^2)\cos\beta\tau - (2\zeta A\beta + \tfrac{3}{4}\mu A^3\beta^3)\sin\beta\tau = \cos\phi\cos\beta\tau - \sin\phi\sin\beta\tau$$

Equating the coefficients of $\cos\beta\tau$ and also of $\sin\beta\tau$ on either side of the equation we obtain the equations

$$(54)\qquad A(1-\beta^2) = \cos\phi$$

$$(55)\qquad 2\zeta A\beta + \tfrac{3}{4}\mu A^3\beta^3 = \sin\phi$$

from which, by noting that

$$\sin^2\phi + \cos^2\phi = 1$$

we can write the following equation

$$(56)\beta^6(9/16\,\mu^2A^4)+\beta^4(1+3\mu\zeta A^2)+\beta^2(4\zeta^2-2)+(1-\frac{1}{A^2})=0$$

It is the real roots of the cubic equation in β^2 which are of the most interest to us. Some information concerning the response curve can be obtained by use of Descartes' rule of signs. First, we note that the coefficient of β^6 is always positive. For $A>1$ there are either two or zero changes of sign giving the possibility of two or zero real positive roots (values of β^2). For $A<1$, there are either one or three changes of sign. Three changes of sign are possible only for negative μ. This would seem to indicate the possibility of three roots for some values of $A<1$, but this was not observed experimentally.

The approximate solution was calculated for the case $\mu=-0.02$, $\zeta=0.20$. The roots of the cubic equation in β^2 were evaluated for various amplitudes by using Newton's method. The experimental values were used as an aid in making a first guess. The results are plotted in Fig. 5.04.

As in the previous case of a cubic spring, the analytic and experimental results do not agree very well for large A. This may be due to the fact that the neglected term is proportional to A^3.

2. Van der Pol's equation

Self-excited oscillations can be obtained with a system having negative linear damping and also a cubic damping term

with a positive coefficient.

For example, consider the electrical circuit described by the equation

$$L\ddot{q} - R\dot{q} + \alpha\dot{q}^3 + \frac{q}{C} = 0$$

or

(57) $$\ddot{q} - \frac{R}{L}\dot{q} + \frac{\alpha}{L}\dot{q}^3 + \frac{q}{LC} = 0$$

Now let

(58) $$\tau = \frac{t}{\sqrt{LC}}$$

(59) $$x = q\left(\frac{\alpha}{LCR}\right)^{\frac{1}{2}}$$

(60) $$\epsilon = \frac{R}{\sqrt{\frac{L}{C}}}$$

Denoting $\frac{d}{d\tau}$ by a prime, there results

(61) $$x'' - \epsilon(x' - x'^3) + x = 0$$

a. Computer circuit

The computer circuit used to study equation (61) is shown in Fig. 5.06.

The negative linear resistance is obtained by using a gain greater than unity in amplifier 1. R' is used to damp the oscillations upon opening the switch.

b. Results

In order to obtain a wide variation in ϵ, changes

were made in the values of L, C and the gain of the AFG-amplifier 2 combination. ϵ was set to the desired value by choosing convenient values for L and C and then setting amplifier 1 to give the correct negative resistance.

$$R = 66\frac{V_{AB}}{V_{AF}} \text{ ohms} \tag{62}$$

where peak to peak voltages are used. The coefficient results from the fact that resistance $R_{AF} = 66$ ohms.

The oscillations for small values of ϵ are approximately sinusoidal as shown in Fig. 5.07 (a) for the case $\epsilon = 0.10$. Fig. 5.07 (b) shows the buildup process which results upon closing switch BC. The phase diagram is shown in Fig. 5.07 (c). (Velocity is the vertical coordinate and displacement is horizontal coordinate.) Note that the limit cycle is approximately circular, indicating a sinusoidal oscillation.

Figs. 5.07 (d), (e) and (f) are for the case $\epsilon = 1.0$. Here the departure from a sinusoidal waveform is quite noticeable. Figs. 5.07 (d) and (e) show the displacement on buildup and steady state. Fig. 5.07 (f) is the phase diagram for this case.

Figs. 5.07 (g), (h) and (i) are for the case $\epsilon = 6.0$. Fig. 5.07 (g) is a plot of displacement vs. time. Note the fast buildup in this case, giving full amplitude on the first oscillation. Velocity vs. time is shown in Fig. 5.07 (h). This curve has the square characteristic usually

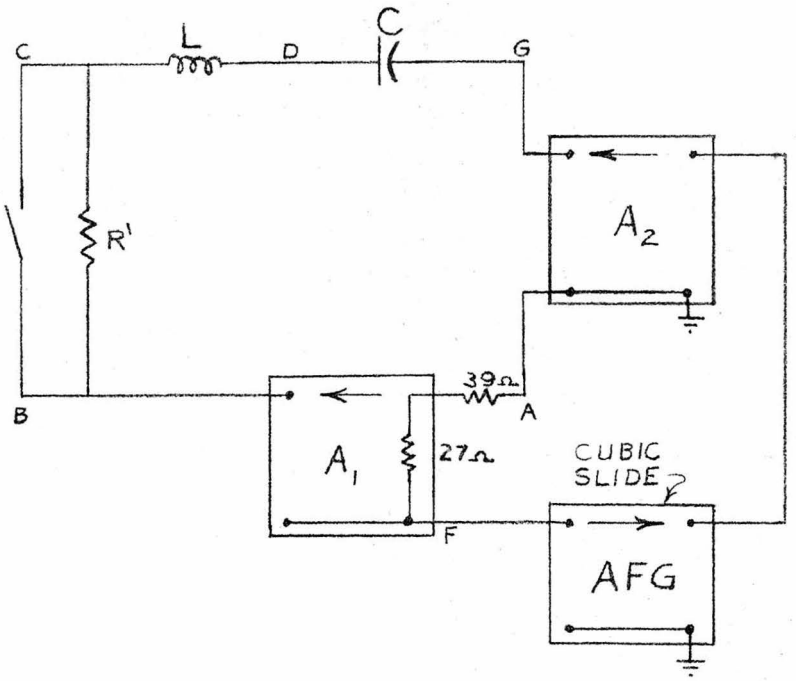

Fig. 5.06

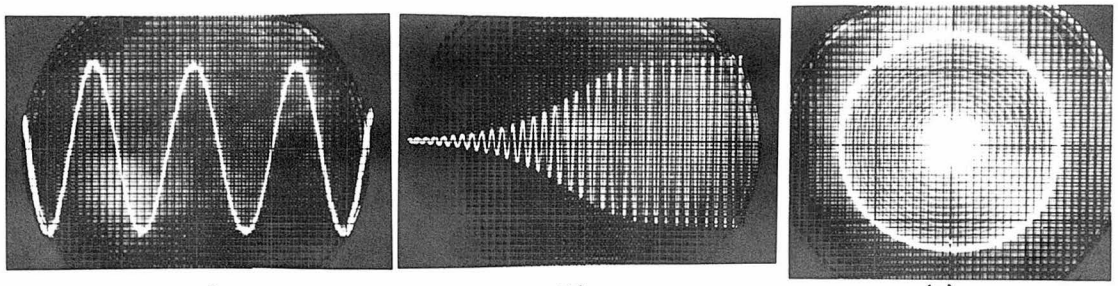

(a) (b) (c)

$\epsilon = 0.1$

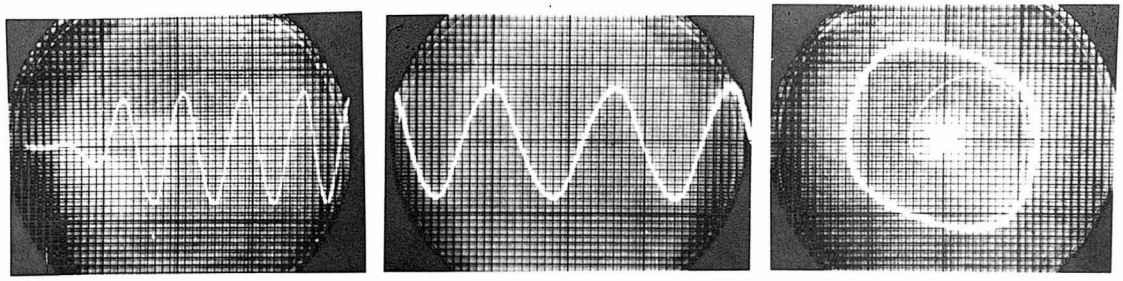

(d) (e) (f)

$\epsilon = 1.0$

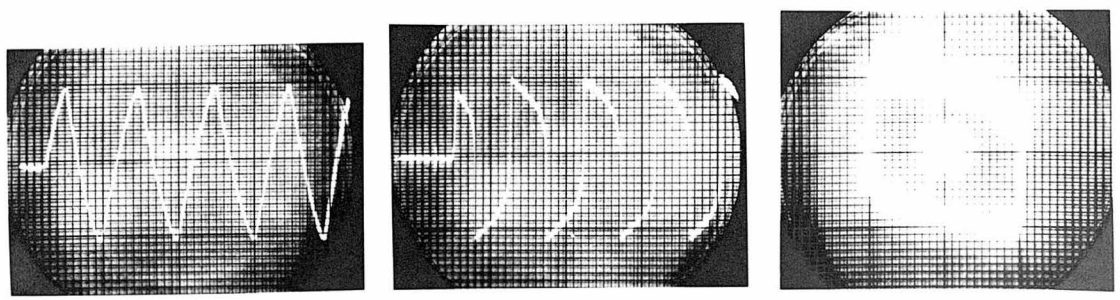

(g) (h) (i)

$\epsilon = 6.0$

FIG. 5.07 SELF-EXCITED OSCILLATIONS

associated with relaxation oscillations. The phase diagram is shown in Fig. 5.07 (i).

PART VI

THE MATHIEU EQUATION

1. The infinitesimal stability of solutions to Duffing's equation

It has been shown in the section on Duffing's equation that the amplitude of the steady state vibration may suddenly change by a large amount even for a very small change of driving frequency. These jumps indicate a region of instability in the $G\beta$ plane. The boundary of the unstable region is shown by the dotted line of Fig. 6.01. Note that this boundary passes through points on the response curves having infinite slope. The above curves are drawn for variations in the parameter γ while ζ retains a constant small value.

Now, following the method of Stoker (9) we shall study the stability properties by means of a variational equation, defining "stability" in the infinitesimal sense. In other words, if we insert $(x + \delta x)$ for x in the differential equation and neglect higher powers of δx we obtain a linear variational equation. If all solutions δx of this equation are bounded, then $x(t)$ is said to be stable. Otherwise, it is unstable.

Let us apply this procedure to the case of Duffing's equation without damping.

$$u'' + u(1 + \gamma u^2) = \cos \beta \tau \tag{63}$$

The variational equation we obtain is

$$\delta u'' + \delta u(1+3\gamma u^2) = 0 \tag{64}$$

Now if we assume that sufficient accuracy can be obtained by using the zero approximation $u_o = A\cos\beta\tau$, the variational equation takes the form

$$\delta u'' + \delta u(1+A^2\ 3/2\ \gamma[1+\cos 2\beta\tau]\ ) = 0 \tag{65}$$

This equation may also be written in the form

$$\frac{d^2(\delta u)}{dz^2} + (\delta + \epsilon\cos z)\ (\delta u) = 0 \tag{66}$$

where

$$z = 2\beta\tau \tag{67}$$

$$\delta = \frac{1}{4\beta^2} + \frac{3\gamma A^2}{8\beta^2} \tag{68}$$

$$\epsilon = \frac{3\gamma A^2}{8\beta^2} \tag{69}$$

This equation is known as the Mathieu equation, and it will have regions of stability and instability corresponding to similar regions in the solution of Duffing's equation.

Thus it may be seen that, although the Mathieu equation is linear, it is useful in the study of the infinitesimal stability of solutions to a nonlinear equation.

This method of analyzing the infinitesimal stability of the first approximations of the periodic solutions is

applicable to a wide variety of nonlinear equations. The variational equation will have variable coefficients but will not necessarily be reducible to Mathieu's equation.

2. Mathieu's equation -- electrical circuit

The computer circuit that is used in the analysis of Mathieu's equation is shown in Fig. 6.02. A linear slide is used in the arbitrary function generator. In this case, then, the arbitrary function generator is being used as an amplifier. A sinusoidal voltage is applied to one multiplier input while the other input is a voltage proportional to the charge on condenser AF. Therefore, the voltage AG is proportional to the charge multiplied by $\cos\omega t$. The gain of amplifier 1 is set to make voltage AB a minimum.

The loop equation for the charge flowing in ABDGA is

$$L\ddot{q} + R\dot{q} + \left(\frac{1}{C} + B\cos\omega t\right)q = 0 \tag{70}$$

The damping term has been included since the actual circuit has a small resistance. Let

$$\tau = \omega t \tag{71}$$

and designate $\frac{dq}{d\tau}$ by q', etc. Then equation (70) becomes

$$q'' + \frac{R}{\omega L}q' + \left(\frac{1}{\omega^2 LC} + \frac{B\cos\tau}{\omega^2 L}\right)q = 0 \tag{72}$$

or

(73) $$q'' + 2\zeta q' + (\delta + \epsilon \cos\tau)q = 0$$

where

(74) $$\zeta = \frac{R}{2\omega L}$$

(75) $$\delta = \frac{1}{\omega^2 LC} = \left(\frac{\omega_o}{\omega}\right)^2$$

(76) $$\epsilon = \frac{B}{\omega^2 L} = CB\left(\frac{\omega_o}{\omega}\right)^2$$

Stability tests were run with the electrical circuit. It was desired to be able to vary the parameters δ and ϵ independently. δ was controlled by changing the frequency of the voltage source connected between busses A and J.

The ratio $\frac{\epsilon}{\delta}$ was read from the dial of the input potentiometer (Helipot) on the arbitrary function generator. The dial was first set to 1.00 and amplifier gains elsewhere in the feedback loop were adjusted to give $\frac{\epsilon}{\delta} = 1$. This was accomplished by opening the feedback loop and comparing the maximum voltage amplitude across DG with the output AE of amplifier 2 when the main loop is driven by a voltage between B and C and the voltage AJ is set to its standard value (0.34 volts). (See Fig. 6.03.) In this case, the voltages BC and AJ were equal in frequency and phase. With proper calibration the ratio $\frac{\epsilon}{\delta}$ can thus be read directly from the setting of the input potentiometer of the arbitrary function generator. A ten-to-one voltage attenuator incorporated in amplifier 2 was used to change the

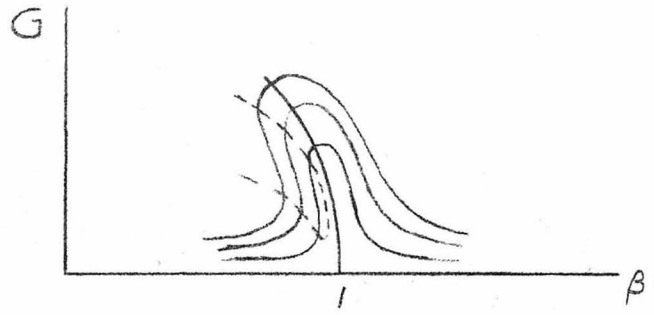

Fig. 6.01

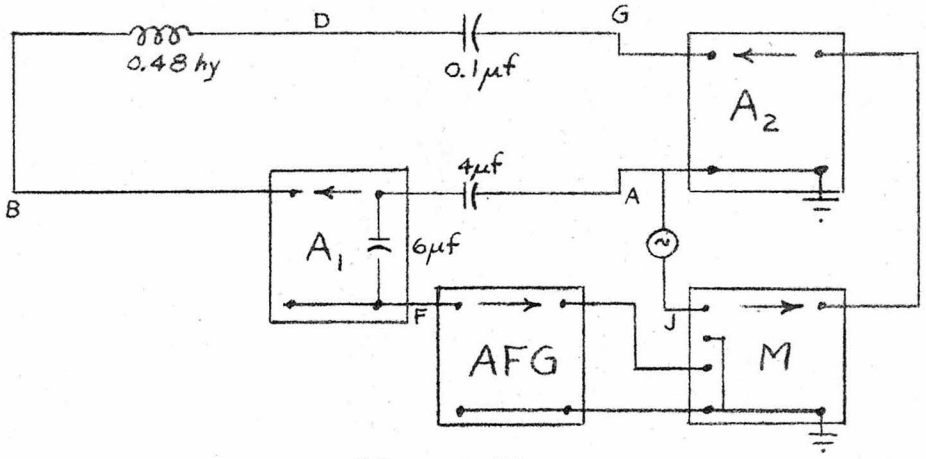

Fig. 6.02

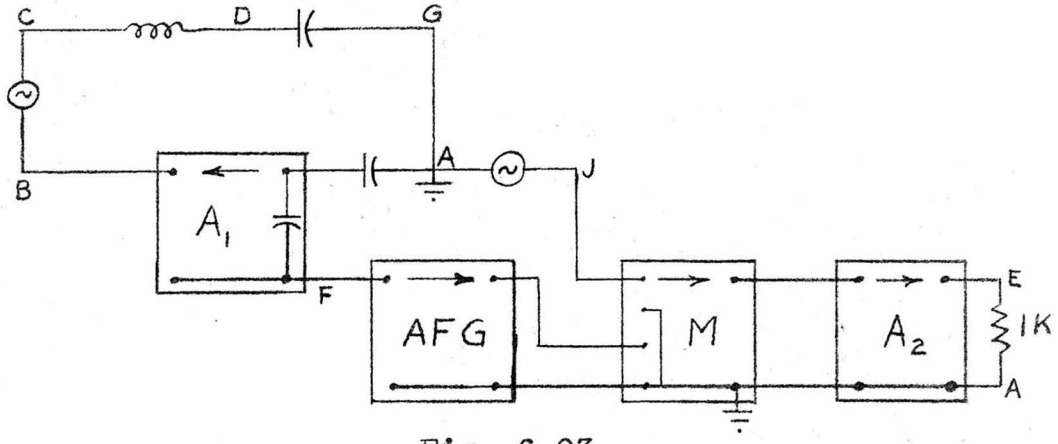

Fig. 6.03

scale of the Helipot readings.

3. Experimental results

Data was taken to determine experimentally the regions of stability in the $\delta\epsilon$ plane. This was obtained by taking limiting values of $\frac{\epsilon}{\delta}$ for various driving frequencies. The results are shown in Fig. 6.04. The boundaries of the regions of stability determined by this means have approximately the same shape as the theoretical boundaries. However, the scale of the ϵ coordinate should be multiplied by about 3/2. There was a small "hysteresis" effect noted in the experimental determinations; i.e., instability occurs at a higher value of $\frac{\epsilon}{\delta}$ than that at which the system returns to stability.

4. Effect of damping

As has been stated previously, the experimental stability determinations were made on a circuit represented by a Mathieu equation modified by the addition of a damping term $2\zeta q'$. If the substitution

$$q = ue^{-\zeta\tau} \tag{77}$$

is made in equation (73), the result is

$$u'' + \left[(\delta - \zeta^2) + \epsilon\cos\tau\right]u = 0 \tag{78}$$

To obtain some indication of the effect of damping, let us calculate the value of $\zeta = \frac{R}{2\omega L}$ for $\left(\frac{\omega_o}{\omega}\right) = 1$ (720 cycles).

Regions of Stability — Mathieu Equation

$$u'' + (\delta + \epsilon \cos\tau)\, u = 0$$

Fig. 6.04

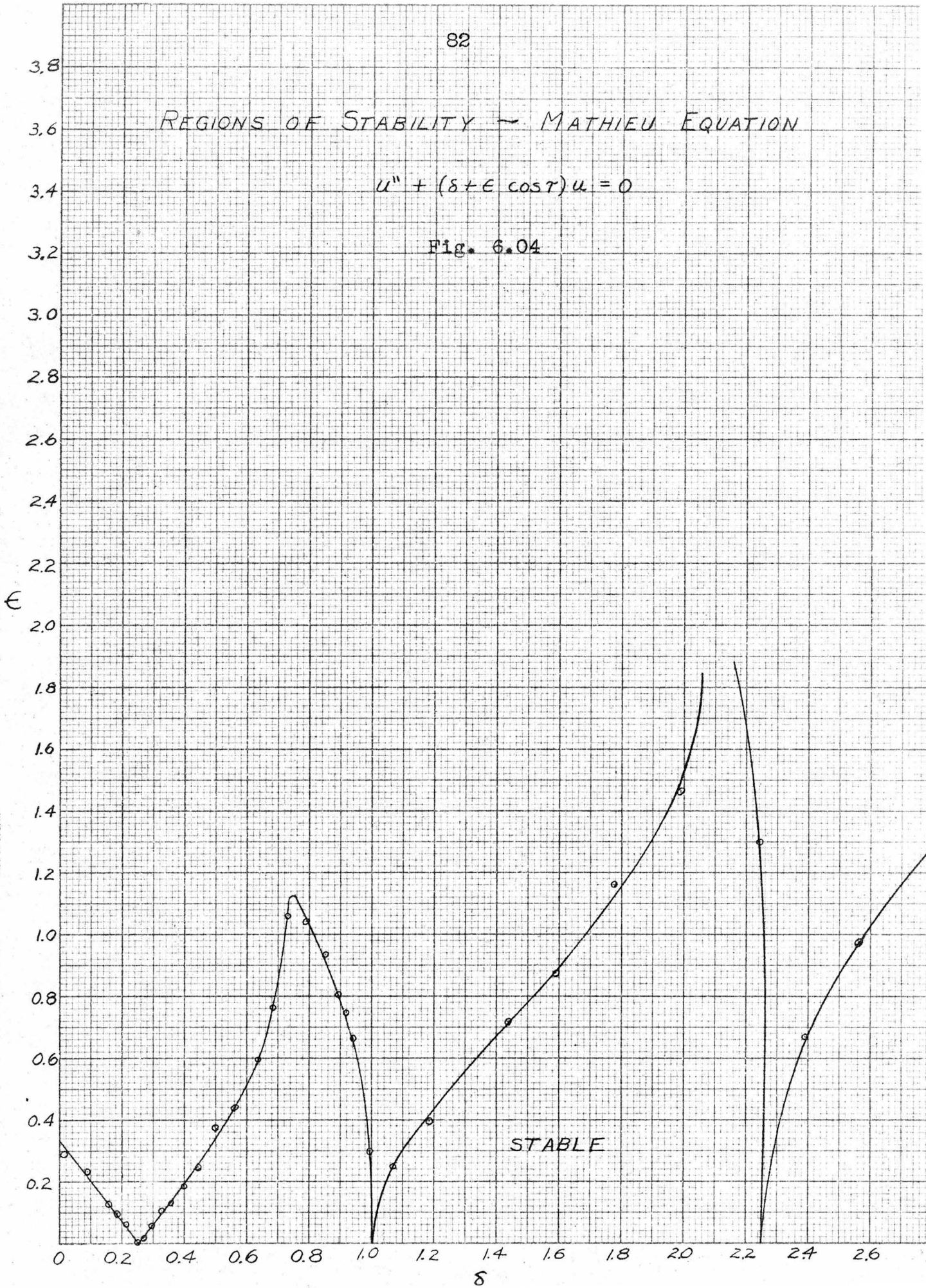

$$R = 28 \ \Omega$$

$$L = 0.48 \text{ hy}$$

Therefore

$$\zeta = \frac{28}{2880\pi(.48)} = 0.00645$$

Since R is roughly proportional to frequency over much of the frequency range used in these experiments, ζ is independent of frequency over all except low values of ω where R is nearly independent of frequency. The correction term is ζ^2, and therefore, the effect of damping is negligible except for small δ. For the case of large ζ, it may be seen that the effect of damping is to shift the operating point to the left in the $\delta\epsilon$ plane. Thus one might think the damping might tend to cause instability, since a shift to the left generally has a destabilizing effect. However, we are not interested in the amplitude of u but rather of $q = ue^{-\zeta\tau}$. Thus u may increase exponentially and be "unstable" while the amplitude of q remains bounded. It is shown by Minorsky (10) that damping causes greater stability as one might expect from energy considerations.

5. Parametric excitation

It might be noted that when instability occurs, the arbitrary function generator saturates due to the driving of the spot to the edge of the slide. Thus the oscillations are limited in amplitude to a reasonable value. Photographs

were taken of the response in the unstable region of the plane.

As the frequency of the excitation was varied, a variety of types of oscillations occurred. (See Fig. 6.05.) Examples of subharmonics, ultraharmonics and ultrasubharmonics are shown.

Figs. 6.05 (a) and (b) show examples of subharmonic oscillations. The period of the response (upper trace) is equal to the period of the free oscillation, but the period of the excitation is smaller by a factor $\frac{1}{n}$ where n is an integer. (Examples of n = 2, 3 are shown.)

An example of ultraharmonic oscillation is shown in Fig. 6.05 (c). In this case the response and excitation both have the same period, but this period is an integral multiple, m, (in this case m = 2) of the natural period.

Examples of ultrasubharmonic oscillations are shown in Figs. 6.05 (d- i). In this type of oscillation, the period of the response is m times the natural period and n times that of the excitation.

Although the experimental work was done for the specific case of Mathieu's equation, studies could be made of systems in which the damping coefficient is also a periodic function of time.

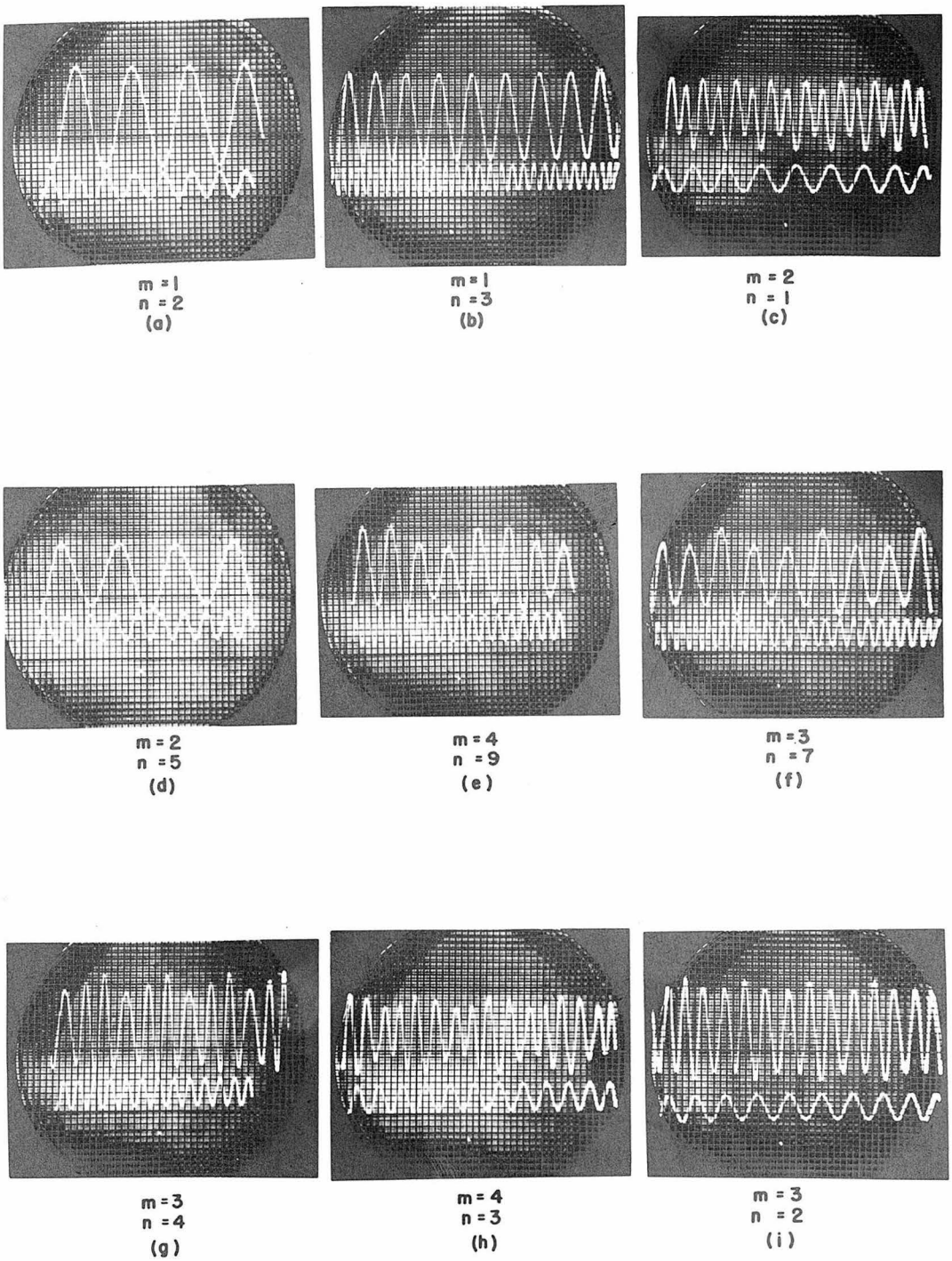

m = 1
n = 2
(a)

m = 1
n = 3
(b)

m = 2
n = 1
(c)

m = 2
n = 5
(d)

m = 4
n = 9
(e)

m = 3
n = 7
(f)

m = 3
n = 4
(g)

m = 4
n = 3
(h)

m = 3
n = 2
(i)

FIG. 6.05 PARAMETRIC EXCITATION

REFERENCES

1. Gardner, M. F. and Barnes, J. L., Transients in Linear Systems, John Wiley and Sons, (1942), Chapt. II.

2. McCann, G. D., Wilts, C. H. and Locanthi, B. N., "Electronic Techniques Applied to Analogue Methods of Computation," Proceedings, IRE, (August, 1949), pages 954-61.

3. MacNeal, R. H., "The Solution of Partial Differential Equations by means of Electrical Networks," Ph D Thesis, California Institute of Technology, (1949).

4. Russell, W. T., "Lumped Parameter Analogies for Continuous Mechanical Systems," Ph D Thesis, California Institute of Technology, (1950).

5. McCann, G. D. and MacNeal, R. H., "Beam Vibration Analysis with the Electric Analog Computer," Journal of Applied Mechanics, vol. 17, (March, 1950).

6. McCann, G. D., Wilts, C. H. and Locanthi, B. N., "Application of the California Institute of Technology Electric Analog Computer to Nonlinear Mechanics and Servomechanisms," Transactions, AIEE, (1949).

7. Buchholz, W., "An Arbitrary Function Generator and Its Application to the Study of Some Nonlinear Systems on the Electric Analog Computer," Ph D Thesis, California Institute of Technology, (1950).

8. McCann, G. D., "The California Institute of Technology Electric Analog Computer," Mathematical Tables and Other Aids to Computation, III, No. 28, (October, 1949).

9. Stoker, J. J., Nonlinear Vibrations in Mechanical and Electrical Systems, Interscience Publishers, (1950).

10. Minorsky, N., Introduction to Non-linear Mechanics, J. W. Edwards, (1947), pages 369-371.